Separation and Purification Technology 360 (2025) 131061

Contents lists available at ScienceDirect

Separation and Purification Technology

journal homepage: www.elsevier.com/locate/seppur

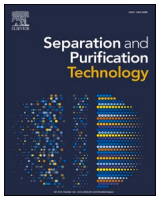

Electrifying distillation – Optimization-based evaluation of internally heat-integrated distillation columns

Momme Adami [1], Kayenat Farheen [1], Mirko Skiborowski [*]

Hamburg University of Technology, Institute of Process Systems Engineering, Am Schwarzenberg-Campus 4, 21073 Hamburg, Germany

ARTICLE INFO

Editor: B. Van der Bruggen

Keywords:
Electrified Distillation
Heat pumps
Vapor recompression
HIDiC
Heat integration
Optimization-based design

ABSTRACT

Improving the energy efficiency of distillation processes is essential for reducing the chemical industry's substantial energy demand and environmental footprint. The use of mechanical heat pumps with compressors is an important asset in this transformation process, as it not only enables the recovery of heat rejected at low temperature, reducing external energy requirements, but also facilitates the electrification of chemical processes and distillation in specific. The necessary temperature lift dictates the required compression rate for the compressor and is therefore of considerable importance for the applicability of mechanical heat pumps. By operating the rectifying and stripping sections of a column at different pressures and enabling heat exchange between the respective sections, temperature lift and compression ratio can be reduced for the so-called Internally Heat-Integrated Distillation Columns compared to mechanical vapor recompression. In order to enable a quick problem specific evaluation of the possible benefits of this concept we propose two novel superstructure models for optimal design, that allow for heat exchange between stages at the same height or arbitrary stages in the rectifying and stripping section, provided a minimum temperature difference is maintained. The respective optimization problems are solved as a series of successively relaxed mixed-integer nonlinear programming problems in GAMS. An automatic stepwise initialization and optimization strategy provides a computationally efficient approach for the determination of optimized designs.

1. Introduction

In order to limit global warming to 1.5 °C, the European Union has set a target of net-zero carbon emissions by 2050 [1]. Nearly 80% of the current greenhouse gas emissions are attributed to energy demand [2]. Distillation is recognized as the most energy intensive process in the chemical industry, accounting for 90–95% of all fluid separations [3]. It is characterized by high-temperature energy demand at the reboiler and low-temperature rejected heat at the condenser, resulting in exergy losses. Distillation is considered the most mature and most widely employed thermal separation technology, being considered as most robust with the ability to handle a wide range of throughputs, feed concentrations and high product purities. Although other nonthermal separation processes, especially membrane separations that completely avoid phase transitions, have showcased considerable improvements in certain applications, it can be shown that all separation processes suffer similar limitations than distillation, when processing large capacities with high purity requirements for both product streams [4]. Therefore it is essential to reduce the energy demand of distillation processes and improve their energy efficiency [5].

For this purpose, several energy integration techniques such as direct heat integration, thermal coupling, and multi-effect distillation have been proposed [6]. Thermal coupling, for instance, implements a bi-directional vapor and liquid transfer instead of intermediate reboilers and condensers between adjacent columns in a column sequence, effectively reducing mixing losses and the required net energy demand. The reduced number of required heat exchangers and the possible implementation as dividing wall column further enables a decreased capital cost [7]. Another option to reduce external heat requirements constitutes direct heat integration between adjacent columns, by adjusting the pressure in at least one of the columns to provide a sufficient temperature difference between the condenser of a column as heat source and the reboiler of another column that constitutes the heat sink. However, all these concepts are only applicable to sequences of multiple distillation columns.

An individual distillation column can be conceptualized as a heat

* Corresponding author.
E-mail address: mirko.skiborowski@tuhh.de (M. Skiborowski).
[1] Contributed equally to the article.

https://doi.org/10.1016/j.seppur.2024.131061
Received 27 September 2024; Received in revised form 10 December 2024; Accepted 11 December 2024
Available online 15 December 2024

engine that transforms the heat duty of the reboiler into separation work performed at the temperature level of the condenser [8]. Accordingly, the individual components in the column are purified, while the temperature decreases along the column height. Heat pumps effectively reverse a part of this process and are an important option to improve the energy efficiency of individual distillation splits, by minimizing the exergy losses that occur during heat transfer in the heat exchangers [9]. Heat-pump assisted distillation can therefore exploit high internal efficiencies of distillation columns, which can yield up to 70% or above for proper feed compositions and potential preheating [10], allowing for overall energy savings of over 80% compared to a simple distillation column [11]. With an increasing share of renewable electricity generation, the use of electrically driven heat pumps for energy integration of distillation columns becomes an even more sustainable choice [2]. However, challenges remain, such as the fluctuating availability of renewable electricity, necessitating complementary solutions including electrical energy storage to ensure continuous operation [12]. Additionally, strategies like demand management and partial-load operation should be considered to enable distillation systems to adjust efficiently based on the varying supply of renewable energy [13].

Heat pumps can be classified into compression heat pumps, absorption heat pumps and hybrid heat pumps [5], of which compression heat pumps are the most widely used in distillation due to the higher coefficient of performance and low investment cost [14]. They operate on the vapor compression cycle, consisting of a compressor, condenser, throttle valve and an evaporator. Several heat pump-assisted distillation concepts have been developed, including mechanical vapor recompression (VRC), bottom flashing, internally heat integrated distillation column (HIDiC), and middle vapor recompression (MiVRC), as illustrated in Fig. 1.

Among these, VRC is the most common concept. In VRC the vapor from the top of the column is compressed to a higher pressure and thus boiling temperature to provide the heating duty in the reboiler by condensation of the compressed vapor [15]. Compared to a conventional distillation column, VRC can save up to 80% of the energy cost, but at higher capital cost due to the expensive compressor [16]. However, since vapor from the top of the entire column needs to be compressed, the temperature increase required in the compressor is the largest possible as it exceeds the temperature difference between the boiling temperatures of the top and bottom products by an additional approach temperature for the heat exchange (see Fig. 1.), resulting in the highest possible compression ratio of the mentioned heat-pump assisted distillation concepts and thus also a high compression duty [11]. Thus, VRC is considered most suitable for close-boiling mixtures for which this temperature difference is small [15]. This is generally valid for all heat pump concepts, as the compressor duty and thus its cost depend on the compression ratio with lower compression ratios being more attractive. Therefore, other concepts for heat pump assisted distillation target a limited temperature lift and compression ratio, by avoiding heat integration between the column top and bottoms streams.

MiVRC is a relatively new concept introduced by Cong *et al.* [17] in 2018. In MiVRC the top vapor from the stripping section is compressed to provide the heat for the reboiler, before being passed to the rectifying section, which is operated at a higher pressure than the stripping section. Due to the condensation in the reboiler only a fraction of the compressed stream is used to provide the heat in the reboiler, while the remaining part is passed as vapor stream to the rectifying section. The condensed stream from the reboiler is combined with the liquid exiting the bottom of the rectifying section. This mixed stream is expanded and subsequently serves as a cooling medium in the condenser. However, to achieve heat integration at the reboiler and condenser while also providing enough vapor for the separation, an additional recycle loop is required which leads to higher internal flow rates. As a result, the stream leaving the condenser becomes two-phase of which the liquid portion serves as reflux to the stripping section, while the vapor phase is recycled through the compressor. Cong *et al.* [17] reported a ~36% lower compression ratio for MiVRC when compared with the VRC for an equal mass fraction feed of benzene-toluene. Due to the increased internal flowrates, the compressor work for the MiVRC is however higher than for VRC, compensating the benefit of lower compression ratio [17].

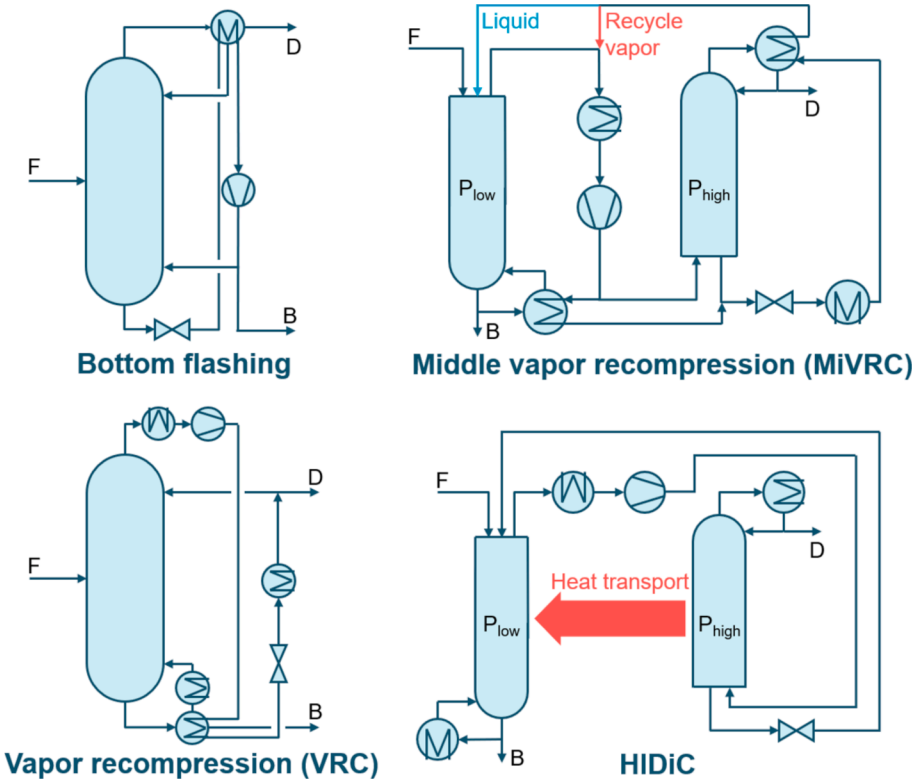

Fig. 1. Flowsheets of heat pump assisted distillation concepts.

Similar to MiVRC, a HIDiC is a type of heat pump assisted distillation technique that uses physically separated column sections [18,19]. However, the concept of a HIDiC is much older and was already proposed as secondary reflux and vaporization distillation column by Mah *et al.* [20] in 1977. The concept of operating the rectifying section at an elevated temperature by intermediately compressing the vapor stream from the stripping section, in order to perform a heat integration, has been proposed even prior to that for gas separation by Haselden in 1958 [21]. The rectifying section is operated at a higher pressure than the stripping section by compressing the vapor from the top of the stripping section in order to transfer heat from the rectifying to the stripping section at either individual heights or continuously, accordingly requiring a lower compression ratio than VRC. The basic concept of a HIDiC is based on the idea of reversible distillation with zero entropy production to minimize exergy losses [22] which would require infinitesimally small heat exchange at zero temperature difference [23] at an infinite number of stages [24]. The irreversibility of a binary distillation system can be illustrated using a McCabe-Thiele diagram, where the gap between the operating lines and the equilibrium curve indicates the degree of irreversibility; the larger the gap, the greater the irreversibility within the system [10]. In the reversible case, the operating line would be an operating curve and coincide with the equilibrium curve [19]. While the use of intermediate heat exchangers reduces the irreversibility and improves the efficiency of the distillation, it does not lower the external energy demand [10].

Unlike MiVRC, where heat integration occurs only at the reboiler and condenser, HIDiC uses intermediate heat exchange between both column sections to reduce the irreversibility by transferring heat from stages in the rectifying section to stages in the stripping section and thus approaches a reversible distillation column with the highest internal efficiency [25]. The vapor from the top of the stripping section is compressed in such a way, that at each stage the temperature in the rectifying section is high enough to evaporate liquid in the stripping section of a corresponding stage. This also results in the simultaneous generation of reflux in the rectifying section from the condensation of vapor, thus theoretically entirely eliminating the need for any external hot or cold utilities after start-up [5]. Because of the low compression ratio due to the smaller temperature lift and low exergy losses resulting from heat integration along the height of the column, the HIDiC is generally considered as a promising electrified distillation alternative to VRC and conventional columns with energy savings of up to 90% [19] up to the point of full heat integration where only a small amount of electricity and no heat needs to be supplied. In practice, a trim condenser or reboiler will be required depending on the specific characteristics of the mixture being separated [26].

There are two main approaches to practical HIDiC implementation. The first approach builds on conventional column shells for both sections with externally located side heat exchangers, which allow for individual sizing, but require additional investment. The second approach focusses on continuous heat transfer along the column height using specialized equipment [19]. The main challenge is to obtain adequate heat transfer area while simultaneously maintaining the separation requirements. Several proposals in literature for this type of design include multi-tube, split, concentric and multi-concentric designs [27]. A pilot plant based on the multi-tube scheme has been constructed and successfully operated under conditions where no external reflux is required [28]. When heat transfer through the wall is not sufficient, special column internals are required. For this purpose, Gadalla *et al.* [27] introduced heat panels between the rectifying and stripping sections, while Marin-Gallego *et al.* [29] tested the performance of a metal foam packing in a concentric HIDiC pilot plant. Despite some initial implementations of HIDiC with continuous heat transfer between the column sections [28,30], the only known industrial implementation of a HIDiC makes use of a small finite number of external heat exchangers and separate column sections [31]. The so-called Super-HIDiC was built by Toyo Engineering in collaboration with Koch-Glitsch [32] for the fractionation of methyl ethyl ketone in the Chiba Factory of Maruzen Petrochemical Co. Ltd. In Japan [31].

In order to quantify possible energy and cost savings over conventional columns or VRC, several methods for the design of a HIDiC have been developed, including graphical methods that do not guarantee optimality [33]. Posed as a mathematical optimization problem, the design of a HIDiC can be stated and solved as a mixed-integer nonlinear programming (MINLP) problem, which builds on the common MESH model for an equilibrium stage and considers a superstructure formulation, which allows for the variable sizing of the individual column sections, specification of operating pressures in the sections, external heat duties and heat transfer between individual stages in the rectifying and stripping section. However, so far most rigorous HIDiC models only consider heat transfer between stages at the same height in both sections [34,35], although this heat transfer strategy is not necessarily most beneficial or even applicable for all separation problems. Using simulation studies based on the method by Gadalla [36], Shenvi *et al.* [24] showed that for separations with asymmetric column temperature profiles, heat transfer between stages that are not at the same height is more advantageous, which is a direct result from the different driving forces along the column height. Only few design methods for HIDiC allow heat transfer between arbitrary stages in the rectifying and stripping section. Shahandeh *et al.* [37] used a genetic algorithm (GA) for the optimization of a HIDiC with a model that allows for variable heat transfer, but the solution of a single optimization problem requires 10 h of computational time, without any mathematical guarantee of optimality. Qiu *et al.* [38] first built a surrogate model from sampling a rigorous simulation model in Aspen Plus on the basis of an initial sampling of 5000 converged simulations, considering different heat transfer scenarios. This enabled a more time-efficient optimization with a GA, at the cost of the initial sampling for data generation. Furthermore, some simplifications of the design problem were considered, including fixation of the compression ratio, number of stages, number of heat exchangers and one of the heat exchange locations were fixed during the optimization. The necessity for an extensive number of simulations and possible problem simplifications are inherent limitations to such simulation-based optimization methods as the simulation effort scales exponentially with the number of decision variables [39]. The successful application of such a simulation-based optimization further relies heavily on the computational robustness of the individual solutions, which can be challenging for process design problems with closed recycles and several inequality constraints [40,41].

A hierarchical combination of individual rigorous simulations and mixed-integer linear programming (MILP) problems for the heat integration was applied by Alcántara-Avila *et al.* [42]. While this segmentation avoids the direct solution of the more complex mixed-integer nonlinear programming (MINLP) problem, the number of stages in both sections is first determined without considering heat integration, limiting the design space during optimization. Another more recent simulation-based optimization approach by Gutiérrez-Guerra and Segovia-Hernández [43], which also relies on simulation in Aspen Plus, implements an iterative strategy with many adjustments in order to improve the convergence of individual simulations and constraint violations. While this approach overcomes some of the previous limitations and builds on the available models and algorithms in Aspen Plus, it requires a rather complex implementation.

The simultaneous optimization of an equation-oriented superstructure model can effectively cope with a large number of decision variables, including the structural and operational degrees of freedom for distillation processes [44]. While such strategies have proven effective for the design of various complex distillation processes [45–49] only few studies on HIDiC design exploit such an optimization approach. Harwardt and Marquardt [15] were the first to present such an approach based on a MINLP formulation of a generalized HIDiC superstructure with two column shells and conventional heat exchangers, aiming at the minimization of the total energy demand or total annual costs (TAC).

The superstructure model of Harwardt and Marquardt [15] considers fixed heat exchanger locations, i.e. heat transfer between specific equilibrium stages in the superstructure, as well as variable reflux and boil-up locations, in order to reduce the relevant number of trays in the individual sections. As indicated in Fig. 2 this approach allows for some flexibility in the design by having a variable number of trays in each section and thereby freely selecting one heat transfer location, while further heat transfer is limited to parallel trays in the resulting configuration. The MINLP problem is solved as a series of continuously relaxed NLP problems according to Kraemer *et al.* [50].

Although a HIDiC can make use of heat integration at each stage, previous studies have shown that the consideration of only few finite internal heat transfer locations has a negligible impact on the external energy demand [15,24] and reduces the investment cost and thus the TAC [34]. Suphanit [34] and Chen *et al.* [51] performed a simulation-based analysis of the optimal location of an individual heat exchanger based on a sensitivity analysis, while keeping all other parameters such as the number of stages fixed. Harwardt and Marquardt [15] implemented an additional constraint for the maximum number of heat exchangers, which is however inherently further limited by the previously described structural limitation of the superstructure model.

To overcome the different limitations of existing design approaches, especially those of restricted heat exchange locations and fixed compression ratios a set of improved equation-oriented superstructure models is proposed, which is further introduced in Section 2. These models build on the work by Harwardt and Marquardt [15], but introduce additional flexibility, in order to enable heat transfer at different heights, considering the important insight provided by the work of Shenvi *et al.* [24]. In order to evaluate the implications of restrictions on valid heat exchanger locations on the performance as well as the computational effort, a superstructure model that restricts heat transfer between stages with the same stage number in each section (cf. Section 2.3.1), as well as a superstructure model in which heat can be exchanged between any stage of the rectifying section and any stage of the stripping section, provided a minimum temperature difference is maintained (cf. Section 2.3.2) are proposed.

The optimization problems are modeled in GAMS as relaxed NLP problems for which either the external energy demand or TAC are minimized. The superstructure model is set up as an equilibrium stage model based on the MESH equations and a preheater before the compressor is considered to counteract possible condensation during compression. The decision variables include the operating pressure of the rectifying section, number of stages in each section, reflux and boil-up ratios, as well as the location and size of internal heat exchangers.

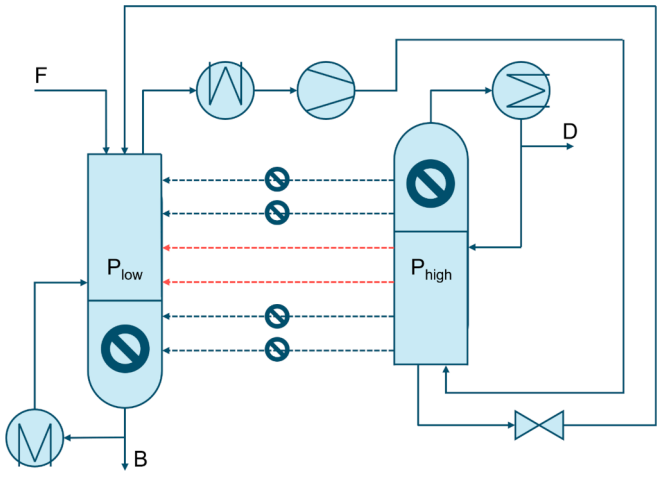

Fig. 2. Model of HIDiC after Harwardt and Marquardt [15] with reduced number of stages showing remaining (red) and eliminated (blue) heat transfer locations. Eliminated stages and heat transfer locations are crossed out. (For interpretation of the references to colour in this figure legend, the reader is referred to the web version of this article.)

Following previous work on the optimization of distillation processes [45,49], a polylithic modeling and solution strategy is developed to solve the complex problem locally by gradually increasing the complexity to provide good initial points each consecutive step, leading to convergence on conventional desktop computers in a few minutes depending on the initial number of stages and utilized heat transfer strategy. The final optimization of the superstructure model is solved as a series of successively relaxed (MI)NLP problems, making use of additional NCP-functions considered in a penalty approach (cf. Section 2), following the strategy of Kraemer *et al.* [50].

The new HIDiC models are applied in optimization studies to first identify the most beneficial heat transfer strategy for HIDiC, considering the competing options of heat transfer along the height of the column or utilizing a finite number of externally located heat exchangers. For further elucidation, the influence of the number of these locations on the external energy demand is evaluated using additional constraints (cf. Section 3.3). After illustrating the benefits of heat transfer at variable heights, the performance of optimal HIDiC designs utilizing variable-height heat transfer is evaluated in comparison to conventional columns and VRC, considering both energetic and economic aspects for close and wide boiling mixtures (cf. Section 3.4).

2. Superstructure optimization models and optimization strategy

The rigorous optimization models for HIDiC are developed as system of equations in GAMS, building on existing models for conventional columns [45] and VRC [49], which are discussed in the following subsections prior to the HIDiC model. All models assume an isobaric operation.

2.1. Optimization model and solution strategy for conventional distillation columns

Fig. 3 (left) shows the superstructure for a conventional distillation column with a single feed and no side streams, for which a detailed description of the model and the solution strategy are described in the work of Skiborowski *et al.* [45]. F, D, and B are the feed, distillate, and bottoms molar flows respectively. R and K are the reflux and boil-up vapor flows, respectively, while x and y are the mole fractions in the liquid and vapor streams, respectively.

Three binary decision variables $b_{F,n}$, $b_{R,n}$, and $b_{K,n}$ are assigned to each stage to decide on the location of the feed flow, reflux flow, and boil-up vapor flow, as shown in Fig. 3 (right) where n is the stage number and L and V are the liquid and vapor molar flows, respectively. Additional summation constraints guarantee that the mass balance is satisfied and that the final decision will be for one location only. In order to solve the resulting MINLP as a series of successively relaxed NLP problems, as proposed by Kraemer *et al.* [50], these decision variables are first relaxed with lower and upper bounds of 0 and 1 respectively, which are tightened in the sequence of NLP problems (cf. Section 2.1), finally providing a solution to the original MINLP problem. Depending on the location of the reflux stream and boil-up vapor flow, some stages from the top of the rectifying section may not have a liquid flow and some stages from the bottom of the stripping section may have no vapor flow. These stages do not contribute to the separation and are considered as non-existent in the scope of equipment sizing and economic evaluation.

Each equilibrium stage is modeled based on the MESH equations. The component specific mass balance for a general stage n and component i in a column is:

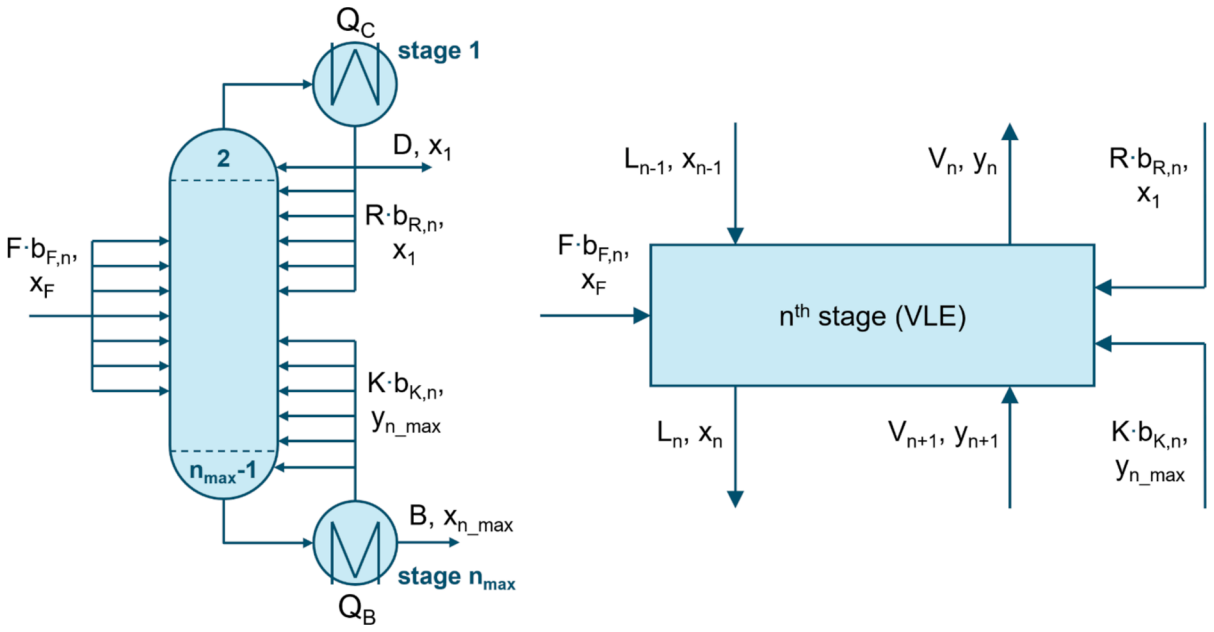

Fig. 3. Superstructure for rigorous optimization of a conventional distillation column (left) and streams entering and leaving a stage (right).

$$L_{n-1}x_{n-1,i} + V_{n+1}y_{n+1,i} + Fb_{F,n}x_{F,i} + Rb_{R,n}x_{1,i} + Kb_{K,n}y_{n_{max},i} = L_n x_{n,i} + V_n y_{n,i}, \quad n \in [2, n_{max}-1] \tag{1}$$

The enthalpy balance for a general stage is similar and described by Eq. (2) with h_n^V and h_n^L as vapor and liquid enthalpy, respectively.

$$L_{n-1}h_{n-1}^L + V_{n+1}h_{n+1}^V + Fb_{F,n}h_F + Rb_{R,n}h_1^L + Kb_{K,n}h_{n_{max}}^V = L_n h_n^L + V_n h_n^V, \quad n \in [2, n_{max}-1] \tag{2}$$

The reboiler and condenser require special treatment. Eq. (3) and Eq. (4) provide the mass and energy balances for the top stage which is representing the condenser with heat duty Q_c.

$$V_2 y_{2,i} = Dx_{1,i} + Rx_{1,i} \tag{3}$$

$$V_2 h_2^V = Dh_1^L + Rh_1^L - Q_C \tag{4}$$

Similarly, Eq. (5) and Eq. (6) present the mass balance and energy balance for the bottom stage, which model the reboiler with heat duty Q_B.

$$L_{n_{max}-1}x_{n_{max}-1,i} = Bx_{n_{max},i} + Ky_{n_{max},i} \tag{5}$$

$$L_{n_{max}-1}h_{n_{max}-1}^L + Q_B = Bh_{n_{max}}^L + Kh_{n_{max}}^V \tag{6}$$

The overall energy and mass balance for the whole column are:

$$F = D + B \tag{7}$$

$$Fh_F + Q_C + Q_B = Dh_1^L + Bh_{n_{max}}^L \tag{8}$$

These equations are accompanied by summation equations for the mole fractions in liquid and vapor:

$$\sum_i x_{n,i} = 1, \quad \sum_i y_{n,i} = 1 \tag{9}$$

The sum of each decision variable across all stages is set to 1 to fulfill the mass balance.

$$\sum_n b_{R,n} = 1, \quad \sum_n b_{K,n} = 1, \quad \sum_n b_{F,n} = 1 \tag{10}$$

The vapor–liquid equilibrium (VLE) calculations involve complex thermodynamics and consist of several non-linear equations with a large number of calculated intermediate variables that are not well-bound and scaled. In order to avoid these complexities, the optimization is performed in a reduced space, by including the VLE and enthalpy computations as implicit functions embedded as external equations implemented in GAMS. Refer to the work of Skiborowski *et al.* [45] for further detail on the external equations. In the current work, all thermodynamic calculations build on DIPPR correlations for the specific heat capacity and heat of vaporization, as well as the extended Antoine equation and the UNIQUAC activity coefficient model. The parameters are provided in the Supporting Information (SI) in section 2.

Due to the discrete decisions on the number of stages or heat exchanger locations and the complex nonlinear thermodynamic models, the MINLP problem for the rigorous optimization of distillation columns is particularly challenging to solve. Previous work has however proven that these problems can be effectively solved to at least local optimality as a series of successively relaxed NLP problems [45,50,52]. Following the polylithic modeling and solution strategy shown in Fig. 4, the complexity of the individual problems is gradually increased while providing good initial values for the next problem. The initial steps are identical for the conventional column, as well as the VRC and HIDiC models, which are discussed in more detail in the subsequent sections.

To provide initial values for the composition and temperature on all stages, at first a feed flash calculation is performed, after which a model with the fixed column structure and mass, equilibrium and summation conditions (MES) is solved, before the full MESH model is considered. Both of these initialization problems already include the purity specifications as inequality constraints. As a last step of the initialization the reboiler duty is minimized, resulting in column design that utilizes all available equilibrium stages while operating at the minimum reflux ratio.

The next step depends on the type of column, while finally all optimization problems consider a techno-economic optimization, based on the minimization of the

$$TAC = C_{op}t_a + \frac{i\cdot(i+1)^t}{(i+1)^t - 1}C_{inv}. \tag{11}$$

The annual operating cost are determined as the product of the hourly operating costs (C_{op}) and the annual operating hours (t_a), which are assumed as 8000 h in this work. The annualized investment cost are

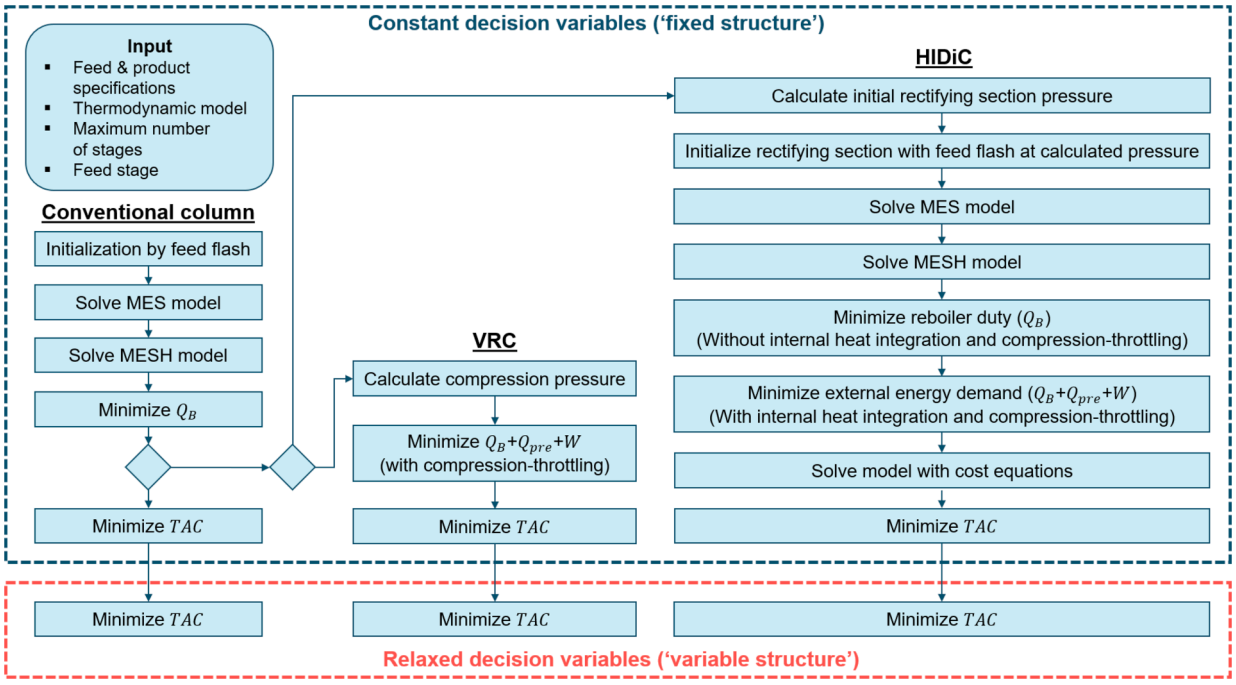

Fig. 4. Optimization strategy for a conventional column, VRC and HIDiC.

determined from the total investment costs (C_{inv}), based on the specific equipment sizing, multiplied by a capital charge factor to consider the interest rate (i) and depreciation time (t) of the plant. An interest rate of 6% and a depreciation time of 10 years are considered in this work. The operating cost depend on the external heating and cooling duties, which are multiplied by the cost of the respective utilities. The investment cost estimation is performed in accordance to Guthrie [53,54] with the module factor method described in the book of Biegler *et al.* [55]. The equipment cost considers the costs of the column shell, tray stack, and heat exchangers with correction factors for design, operating conditions and material. The respective equipment cost correlations are provided in the SI in section 3.

The actual number of stages n_{actual} in the column is calculated by subtracting all stages above the reflux tray and all stages below the boil-up tray from the maximum number of stages n_{max} [50]. The variable $b_{R\_Sum_n}$ is equal to 1 for all stages from the boil-up tray to the reboiler and the variable $b_{K\_Sum_n}$ for all stages from the condenser to the reflux tray. Therefore n_{actual} is corrected by (+2) to make-up for the boil-up and reflux tray.

$$b_{R\_Sum_n} = \sum_{j \geq n}^{n_{max}} b_{R,j} \tag{12}$$

$$b_{K\_Sum_n} = \sum_{j=1}^{n} b_{K,j} \tag{13}$$

$$n_{actual} = n_{max} - \sum_{n=1}^{n_{max}} \left(b_{R_{Sum n}} + b_{K_{Sum n}} \right) + 2 \tag{14}$$

The column shell and tray costs depend on the diameter D_{column} of the column, calculated using Eq. (15), based on the largest vapor flow within the column. In Eq. (15), T is the temperature, R_{gas} the universal gas constant, M_i the molar mass of component i and p the column pressure.

$$D_{column} \geq \sqrt{\frac{4 \cdot V_n}{\pi \cdot 2Pa^{0.5}} \sqrt{\frac{R_{gas} T_n \sum_i y_{n,i} M_i}{p}}}, \quad n \in [2,\, n_{max} - 1] \tag{15}$$

The column height is calculated from the actual number of stages with the actual height of a single tray h_{tray} taken as 0.5 m and an assumed extra clearance space h_{extra} of 4 m, in accordance with Kossack *et al.* [56].

$$H = h_{tray} \cdot n_{actual} + h_{extra} \tag{16}$$

All cost parameters for equipment assumed as stainless steel are taken from Biegler *et al.* [55, pp. 117–134] and a heat transfer coefficient of 1.135 kW/(m^{2}K) is considered for all heat exchangers [55, pp. 114–115].

During all steps of the initialization (blue box in Fig. 4), the maximum number of stages defined for the superstructure is used and further referred to as 'fixed structure'. In the final step during the TAC minimization, the feed, reflux, or boil-up locations are released, which is referred to as 'variable structure'. The final MINLP solution is derived by solving a series of increasingly constrained continuous NLP problems for which the three discrete decision variables are relaxed to continuous values between 0 and 1. Additional Fischer–Burmeister functions, which are non–linear complementary problem (NCP) functions, are added as penalty terms to the objective function, as described by Skiborowski *et al.* [45]. Eq. (17) represents the modified objective function where $p_{F,n}$, $p_{R,n}$, and $p_{K,n}$, are the penalty terms for the relaxed feed, reflux and the boil-up decision variables respectively for stage n.

$$obj_{modified} = TAC + M \cdot \left(\sum_n p_{F,n} + \sum_n p_{R,n} + \sum_n p_{K,n} \right) \tag{17}$$

The penalty terms for the decision variables have a value greater than zero for stages where the value for that decision variable is neither 0 nor 1, thus adding a penalty to the objective function for the non-discrete value of the decision variable for each stage. The penalty weighting factor M is increased by a factor of 10 in a series of successive NLP optimizations, gradually increasing the impact of the penalty terms on the objective function. The iterations are aborted when all three decision variables are either 1 or 0 for each stage of the column.

2.2. Optimization model and solution strategy for VRC

The rigorous optimization model for a VRC is adapted from the work

of Waltermann and Skiborowski [48] and builds on the superstructure model of the conventional column. The superstructure including compression, throttling and heat integration for VRC is shown in Fig. 5.

Following the same initialization steps for a conventional column, the necessary compression ratio for the VRC is determined from a flash computation with an additional constraint on the bubble point temperature of the compressed vapor ($T_{compressedvapor}$), which is required to be higher than the boiling temperature of the bottoms stream ($T_{n_{max}}$) and a minimum temperature difference ΔT_{min} for heat transfer:

$$T_{compressedvapor} \geq T_{n_{max}} + \Delta T_{min} \tag{18}$$

The overall energy balance of the distillation column is modified to include compression and throttling for the open heat pump:

$$Fh_F + Q_B + Q_{aux} + Q_{pre} + W = Dh_1^L + Bh_{n_{max}}^L \tag{19}$$

Here, Q_{pre} is the heating duty in the preheater to avoid condensation in the compressor, Q_{aux} is the cooling duty in the auxiliary condenser for condensation of the vapor formed during throttling to a saturated liquid and W the compressor duty. The condenser and reboiler energy balances are also modified to include the additional duties from heat integration in VRC. Q_{HI} is the energy release by the condensation of the compressed vapor during the heat integration, V_2 is the molar vapor flow through the compressor and the specific enthalpy h_{HI}^l is the enthalpy of the saturated high-pressure liquid leaving the integrated heat exchanger.

$$V_2 h_2^V + Q_{aux} + Q_{pre} + W = Dh_1^L + Rh_1^L + Q_{HI} \tag{20}$$

$$Q_{HI} = V_2 \cdot \left(h_{HI}^l - h_{comp,out}^V\right) \tag{21}$$

$$Q_{aux} = V_2 \left(h_2^l - h_{HI}^l\right) \tag{22}$$

$$L_{n_{max}-1} h_{n_{max}-1}^L + Q_{HI} + Q_B = Bh_{n_{max}}^L + Kh_{n_{max}}^V \tag{23}$$

The compression work W is calculated from the difference of vapor enthalpies at the inlet $h_{comp,in}^V$ and outlet $h_{comp,out}^V$ of the compressor

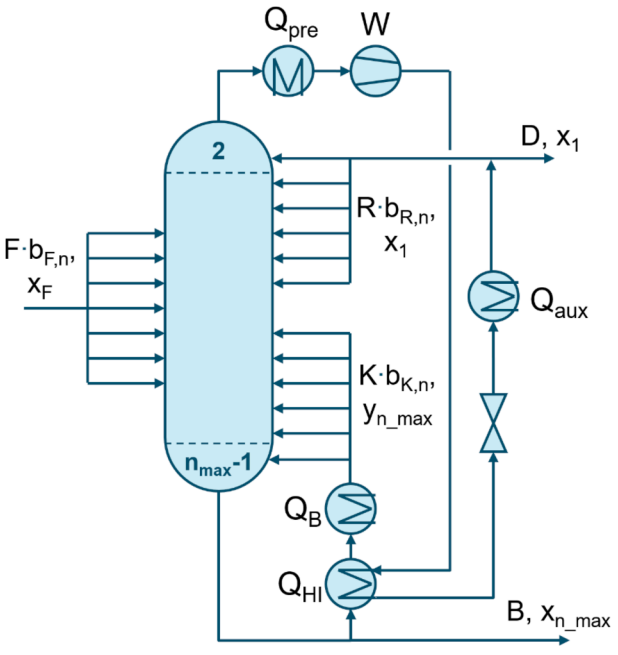

Fig. 5. Superstructure for rigorous optimization of a distillation column with VRC.

$$W = V_2 \left(h_{comp,out}^V - h_{comp,in}^V\right). \tag{24}$$

Following the work of Harwardt and Marquardt [15], the compression is modeled by the isentropic relation for an ideal gas between the input temperature $T_{comp,in}$ and the output temperature $T_{comp,out}$, which is calculated based on the temperature of an isentropic compression

$$T_{comp,isentropic,out} = T_{comp,in} \cdot \left(\frac{p_{out}}{p_{in}}\right)^{\frac{\kappa-1}{\kappa}}, \tag{25}$$

where κ is the isentropic coefficient, calculated from the universal gas constant R_{gas} and the specific heat capacity c_p as

$$\kappa = \frac{c_p}{c_p - R_{gas}}. \tag{26}$$

Assuming an isentropic efficiency $\eta_{isentropic}$ of 80%, the output temperature for a polytropic compression can be determined from the definition of the efficiency

$$\eta_{isentropic} = \frac{\Delta h_{isentropic}}{\Delta h} = \frac{c_p \cdot (T_{comp,isentropic,out} - T_{comp,in})}{c_p \cdot (T_{comp,out} - T_{comp,in})}, \tag{27}$$

for which combination of Eq. (25) and Eq. (27) yields the equality constraint for the computation of

$$T_{comp,out} = T_{comp,in} \cdot \left(1 + \frac{1}{\eta_{isentropic}} \left(\left(\frac{p_{out}}{p_{in}}\right)^{\frac{\kappa-1}{\kappa}} - 1\right)\right). \tag{28}$$

Dry compression is ensured by an inequality constraint

$$T_{compressed\ vapor} \geq T_{sat} \tag{29}$$

on the temperature after compression in relation to the temperature of the saturated vapor at increased pressure (T_{sat}). If preheating is required, the preheating duty is calculated as

$$Q_{pre} = V_2 \cdot \left(h_{comp,in}^V - h_2^V\right). \tag{30}$$

The investment cost of the compressor is calculated based on its compression duty as laid out in the supplementary information. The electricity cost and the compression duty determine its operating cost. The cost of the auxiliary condenser, preheater and heat exchanger for heat integration is considered based on the respective heat exchanger area, similar to the reboiler and condenser, for which the areas are smaller compared to the conventional column.

As illustrated in Fig. 5, the VRC model is first optimized with a fixed column structure for minimum external energy demand, evaluated as the sum of the reboiler duty, the preheating duty and the compression duty, and consecutively for minimum TAC. Afterwards the same solution strategy as for a conventional column is applied to determine the MINLP solution from a sequence of successively relaxed NLP problems.

2.3. Optimization model and solution strategy for HIDiC

The superstructure for HIDiC is shown in Fig. 6. The feed enters the stripping section at the topmost stage. The actual number of stages in both sections remains variable through the reflux and boil-up decision variables with a fixed feed stage, but the number of stages in each section cannot be increased beyond the initial value. Therefore, especially for close-boiling mixtures, a sufficiently high number of stages must be initially defined. To reduce the degrees of freedom further, only the rectifying section pressure is varied and the stripping section pressure is fixed to 1 atm in this work, which can however be adapted without any problem, if required.

Two different model formulations are considered for the HIDiC, considering either same-height heat transfer only (cf. Fig. 6, left), as e.g.

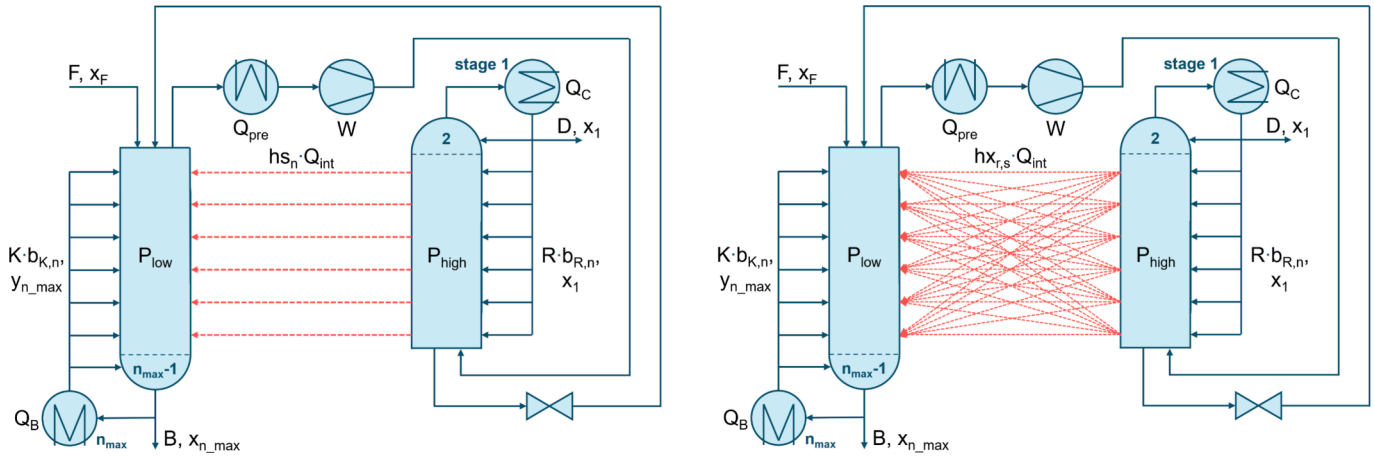

Fig. 6. Superstructures for rigorous optimization of HIDiC with same-height (left) and variable-height (right) heat transfer.

required for equipment integrated designs, or variable-height heat transfer (cf. Fig. 6, right), where heat transfer is indicated by dashed lines for all possible links. In the case of variable-height heat transfer, heat can be transferred from any rectifying section stage to any stripping section stage, given a sufficient driving force, including the possibility of heat transfer between one and multiple stages. For the same-height heat transfer model, only the relative position of the rectifying and stripping section can be determined during optimization, while heat transfer is limited to stages at the same height in each of the sections in the initial superstructure model.

The solution strategy for both HIDiC models also builds on the strategy for a conventional column, as shown in Fig. 4. Similar to the VRC design an initial value for the rectifying section pressure is obtained with the temperature constraint in Eq. (18), considering that the vapor stream from the feed stage is compressed. Next, the rectifying section composition and temperature is initialized with a feed flash at the determined high pressure, followed by solving the MES and MESH equations consecutively for the entire column.

Afterwards, the reboiler duty is minimized for the split column with the compressor without considering any internal heat integration. During this step, two constraints ensure that the temperature in the rectifying section is higher than the temperature in the stripping section for stages that are at the same height. Eq. (18) limits the rectifying section pressure such that the bubble point temperature of the compressed stream is higher than the dew point temperature of the bottoms stream. An additional equation

$$T_1 \geq T_{n_F} + \Delta T_{min} \tag{31}$$

ensures that the distillate temperature (T_1) is greater than the temperature at the feed stage (T_{n_F}), with a minimum temperature difference (ΔT_{min}) considered in both equations. Because separation usually gets more difficult with increasing pressure [57], it is expected that a pressure close to the smallest possible value is chosen.

Internal heat integration and compression and throttling equations are added next. Compression and throttling are similar to VRC, but the vapor leaving the feed stage is compressed and no auxiliary condenser is required. The total energy balance for HIDiC is described by Eq. (32).

$$Fh_F + Q_B + Q_C + Q_{pre} + W = Dh_1^L + Bh_{n_{max}}^L \tag{32}$$

Similar to the distribution of the feed, reflux and boil-up flows, internal heat transfer is represented by dimensionless heat transfer decision variables hr_n and hs_n for the rectifying and stripping sections, respectively, which define the fraction of the overall internally transferred heat Q_{int}, which is withdrawn or transferred to a stage n in either section. The sum of these variables

$$\sum_{n=2}^{n_F-1} hr_n = 1, \quad \sum_{n=n_F}^{n_{max}-1} hs_n = 1, \tag{33}$$

across all stages of the respective section is 1, while each individual decision variable has a lower and upper bound of 0 and 1, respectively. The heat transfer variables are included in the energy balance for both sections. The energy balance for a normal stage in the rectifying section

$$L_{n-1}h_{n-1}^L + V_{n+1}h_{n+1}^V + Rb_{R,n}h_1^L = L_n h_n^L + V_n h_n^V + hr_n \cdot Q_{int}, \quad n \in [2, n_F - 1] \tag{34}$$

is extended by $hr_n \cdot Q_{int}$ as the heat removed from the stage in the rectifying section for internal heat transfer. Similarly, the modified energy balance for a normal stage in the stripping section has an additional term $hs_n \cdot Q_{int}$ for the received heat

$$L_{n-1}h_{n-1}^L + V_{n+1}h_{n+1}^V + Kb_{K,n}h_{n_{max}}^V + hs_n \cdot Q_{int} = L_n h_n^L + V_n h_n^V, \quad n \in [n_F, n_{max} - 1]. \tag{35}$$

The modified energy balance for the stage above the feed, holds a similar term and a modified enthalpy h_{comp}^V, which accounts for the compressed vapor

$$L_{n_F-2}h_{n_F-2}^L + V_{n_F}h_{comp}^V + Rb_{R,n_F-1}h_1^L = L_{n_F-1}h_{n_F-1}^L + V_{n_F-1}h_{n_F-1}^V + hr_{n_F-1} \cdot Q_{int}. \tag{36}$$

The mass and energy balance for the feed stage are also slightly modified due to the column split and the internal heat integration

$$L_{n_F-1}x_{n_F-1,i} + V_{n_F+1}y_{n_F+1,i} + Fx_{F,i} + Kb_{K,n_F}y_{n_{max},i} = L_{n_F}x_{n_F,i} + V_{n_F}y_{n_F,i} \tag{37}$$

$$L_{n_F-1}h_{n_F-1}^L + V_{n_F+1}h_{n_F+1}^V + Fh_F + Kb_{K,n_F}h_{n_{max}}^V + hs_n \cdot Q_{int} = L_{n_F}h_{n_F}^L + V_{n_F}h_{n_F}^V \tag{38}$$

While these equations apply equally for the both HIDIC models, providing a large flexibility, further constraints for the explicit heat transfer links in the variable-height or same–height heat transfer model are discussed in the following subsections 2.3.1 and 2.3.2.

2.3.1. Same-height heat transfer

In the same-height heat transfer model, a direct link between the respective stages in each section is established, by requesting that the heat transfer variable for a stage in the rectifying section is equal to its counterpart for the stripping section at the same height. This is ensured by adding the actual number of rectifying stages $n_{rectifiying\_actual}$ to the index of the heat transfer variable for the stripping section stages. In the fixed structure, it is equal to the initial number of rectifying stages.

$$hr_n = hs_{n+n_{rectifying\_actual}}, \quad n \in [2, n_F - 1] \tag{39}$$

An additional inequality constraint

$$\left(T_n - T_{n+n_{rectifying\_actual}} - \Delta T_{min}\right) \cdot hr_n \geq 0, \quad n \in [2, n_F - 1] \tag{40}$$

is used to ensure that heat transfer occurs only between stages where a minimum temperature difference ΔT_{min} is satisfied. Here, T_n is the temperature of a stage in the rectifying section, while $T_{n+n_{rectifying\_actual}}$ is the temperature of a stage in the stripping section at the same height.

Since the left side of this constraint must be either greater or equal zero, whenever the temperature difference between the rectifying and stripping stages is less than the defined temperature difference, the heat transfer factor hr_n for that stage is forced to be zero. This ensures that heat is only transferred between stages with the required minimum temperature difference.

When optimizing the variable structure in later steps, using the initial number of rectifying stages no longer ensures heat transfer between stages at the same height, because stages are removed from both sections when successively penalizing non-discrete values of the decision variables. Thus, the actual number of rectifying stages must be used during each iteration. Relational operators cannot be used with endogenous variables in GAMS because all equations are solved simultaneously. Instead, the actual number of rectifying stages is implemented as a variable calculated with Eq. (41) and rounded in each iteration, since the result is not necessarily a discrete value.

After discrete values for reflux and boil-up positions are determined, an additional optimization is performed with the updated number of rectifying stages.

$$n_{rectifiying\_actual} = n_F - \sum_n b_{R\_Sum_n} \tag{41}$$

The optimization model is consequently different from that proposed by Harwardt and Marquardt [15], which considered fixed links between column stages in the initial superstructure. Both models are however limited in the possible heat transfer links and another disadvantage of this strategy is the necessary update of the actual number of stages in each section that is only performed between optimizations, such that it is possible that a better solution could be found with a more dynamic update.

2.3.2. Variable-height heat transfer

To allow for flexible heat transfer between one and multiple stages, a third heat transfer variable $hx_{r,s}$ is introduced with lower and upper bounds of 0 and 1 respectively. It defines specific relative amount of heat transfer between an individual pair of stages in the rectifying section (r) and the stripping section (s). Summing over all stages of the rectifying section only changes the value of 's' and describes the entire relative amount of heat transferred from that stage which is equal to

$$hr_n = \sum_{s=n_F}^{n_{max}-1} hx_{r,s}, \quad r = n \forall n \in [2, n_F - 1]. \tag{42}$$

A similar constraint holds for a stage in the stripping section where the value of 's' remains the same and only 'r' varies, in which case the sum is equal to

$$hs_n = \sum_{r=2}^{n_{F-1}} hx_{r,s}, \quad s = n \forall n \in \left[n_F, n_{max} - 1\right]. \tag{43}$$

The inequality constraint used to ensure that heat transfer only occurs between stages with at least a minimum temperature difference is consequently modified to

$$(T_r - T_s - \Delta T_{min}) \cdot hx_{r,s} \geq 0, \quad r \in [2, n_F - 1], \quad s \in [n_F, n_{max} - 1] \tag{44}$$

2.3.3. Optimization of HIDiC for total external energy duty and total annualized cost

Independent of the specific HIDiC model, the model is first solved for minimum total external energy demand (Q_{tot}), which includes the duty of the reboiler, preheater and electrical work for the compressor

$$minQ_{tot} = Q_B + Q_{pre} + W. \tag{45}$$

For the subsequent TAC minimization, the equipment costs need to be determined. The operating costs are calculated identical to VRC, except that the HIDiC does not require an auxiliary condenser. The investment cost of the internal heat exchangers is estimated based on the implementation with conventional external heat exchangers and heat transfer coefficient U. Their area A_{Int_HX} is calculated using an arithmetic temperature difference of the respective stages instead of logarithmic mean temperature differences to simplify the model.

$$A_{Int\_HX_n} \cdot \left(T_n - T_{n+n_{rectifiying\_actual}}\right) = hr_n \cdot Q_{int} \cdot U, \quad n \in [2, n_F - 1] \tag{46}$$

While this assumption is appropriate for close boiling mixtures it should be carefully evaluated for general mixtures and a modification including e.g. the approximation of Chen [58] may be introduced for a more accurate computation of the heat exchanger area. This would however only require a small modification of the presented model. Both column shell diameters are calculated separately based on the maximum vapor flowrate occurring in the respective section, similar to the diameter calculation of a conventional column.

$$D_{rectifying} \geq \sqrt{\frac{4 \cdot V_n}{2\pi \cdot Pa^{0.5}} \sqrt{\frac{R_{gas} T_n \sum_i y_{n,i} M_i}{p_{rectifying}}}}, \quad n \in [2, n_F - 1] \tag{47}$$

$$D_{stripping} \geq \sqrt{\frac{4 \cdot V_n}{2\pi \cdot Pa^{0.5}} \sqrt{\frac{R_{gas} T_n \sum_i y_{n,i} M_i}{p_{stripping}}}}, \quad n \in [n_F, n_{max} - 1] \tag{48}$$

The actual number of stages of both sections is determined with (41) and (49) and the height of each shell calculated identically to a conventional column with an extra clearance space of 2 m.

$$n_{stripping\_actual} = n_{max} - n_F - \sum_1^{n_{max}} b_{K\_Sum_n} \tag{49}$$

The equipment sizing and cost models are first evaluated for the initial design to provide initial values for every variable. Building on the result from the external energy minimization, heat is transferred at a large number of locations since there is no cost attributed to heat exchangers. The initial value for the internal heat exchanger area at each stage is calculated assuming same–height heat transfer regardless of the actual heat integration scenario. In the case of variable-height heat transfer, the heat exchanger area of all other possible connections is initialized to zero. The cost of the internal heat exchangers is then initialized for each stage based on the initialization of the heat exchanger area.

The variable structure optimization strategy is similar to a conventional column with the difference of a fixed feed stage for HIDiC, so only the penalty terms for reflux and boil-up positions are required. Due to the many degrees of freedom, convergence is difficult in the variable structure for HIDiC, especially in the case of variable-height heat transfer, since there is one decision variable per stage and the number of variables $hx_{r,s}$ scales quadratically with the number of stages per section (e.g. 100 decision variables and 2500 variables $hx_{r,s}$ for 50 stages in each section). To aid convergence, the number of stages in each section obtained for a conventional column is used to initialize and select upper bounds for the variable structure decision variables of HIDiC. With the reduced driving forces for HIDiC, at least the same number of stages as for a conventional column should be required, such that the superstructure model should provide a sufficient excess of stages compared to

a simple column design. Due to the local optimization of the complex nonconvex optimization problem modification of the bounds and initial point may be required to obtain good solutions, which can be efficiently tested based on the proposed optimization approach. Such modifications may further be automated in the future by integrating the local optimization approach in a hybrid optimization strategy [59,60].

Heat integration is limited to stages which contribute to the separation and therefore are between the reflux and boil-up positions as shown in Fig. 7. If

$$b_{R\_Sum_{n+1}} + hr_n \leq 1, \quad n \in [2, n_F - 1] \tag{50}$$

is actually equal to 1, then hr_n must be zero to satisfy the inequality. This ensures that no heat transfer occurs from the stages located above the reflux position. A similar inequality constraint

$$b_{K\_Sum_{n-1}} + hs_n \leq 1, \quad n \in [n_F, n_{max}] \tag{51}$$

is used to ensure that only stages above the boil-up vapor position can receive heat in the stripping section. If $b_{K\_Sum_n}$ is 1, then hs_n must be zero to satisfy the inequality.

2.3.4. Constraints on the number of internal heat exchange locations

When minimizing the total external energy demand, heat transfer at many stages is utilized and the individual amount of transferred heat is often small. From an equipment design and cost perspective, it is beneficial to only transfer heat at a few positions, which is already considered when minimizing TAC. However, to assess the energy saving potential of HIDiC with a particular number of internal heat exchangers, the number of heat transfer locations in can be constrained during minimization of the total external duty.

To track and limit the presence of internal heat exchangers without implementing binary variables that make the solution of the model more challenging, a continuous variable nhx_n with a lower bound of 0 and an upper bound of 1 is introduced for each stage. In accordance with

$$(nhx_n - 1)\cdot(nhx_n + hr_n) \geq 0, \quad n \in [2, n_F - 1] \tag{52}$$

it takes the value of 1 to indicate the presence of heat transfer ($hr_n \neq 0$) and 0 otherwise.

To ensure that nhx is zero when there is no heat transfer ($hr_n = 0$), a Big-M constraint is applied

$$(1000\cdot hr_n) - nhx_n \geq 0, \quad n \in [2, n_F - 1] \tag{53}$$

A large constant (M = 1000) is chosen to effectively make nhx_n zero in the absence of heat transfer. This method inadvertently sets a lower limit for heat transfer, which aligns with the design goal to focus on significant heat exchange locations. The sum of nhx_n across all rectifying section stages is equal to a discrete number of internal heat exchange locations NHX for same-height heat transfer.

$$NHX = \sum_{n=2}^{n_F-1} nhx_n \tag{54}$$

Constraints (52) and (53) are only valid for same-height heat transfer, but equally applicable for variable-height heat transfer by replacing hr_n with $hx_{r,s}$ and nhx_n with $nhx_{r,s}$. The number of heat exchange locations for variable-height heat transfer is

$$NHX = \sum_{r=2}^{n_F-1} \sum_{s=n_F}^{n_{max}-1} nhx_{r,s}. \tag{55}$$

The model without constraints on the number of internal heat exchangers is optimized first to obtain suitable initial values before optimizing with these constraints.

3. Case studies

This chapter presents optimization results for exemplary case studies to evaluate the performance of the individual model formulation and solution strategies and the competing heat integration concepts. All case studies consider a saturated liquid feed of 10 mol/s, a minimum temperature difference of 10 K in heat exchangers, unless otherwise stated. All product purities are constrained to be at least 99% and the considered utility costs are listed in Table 1. All optimizations are performed with GAMS 34.3.0 on a desktop PC with an Intel i7-6700 CPU, using SNOPT for the solution of the NLP problems.

Section 3.1 first presents a comparative evaluation of the same-height heat transfer and variable-height heat transfer models, while Sections 3.2 and 3.3 evaluate the competing concepts of continuously integrating heat along the column height in the HIDiC with a restricted number of external heat exchangers, before Section 3.4 finally evaluates the most attractive heat integration strategy for HIDiC in respect to the required energy and economic performance in comparison with

Table 1
Utility cost used in this work, after Turton *et al.* [61, p. 231].

Utility	Cost
Steam (6 bar, 433.15 K)	29.29 €/t = 14.05 €/GJ
Cooling water (303.15 K, ΔT = 10 K)	0.0148 € /t = 0.354 €/GJ
Electricity	0.06 €/kWh = 16.8 €/GJ

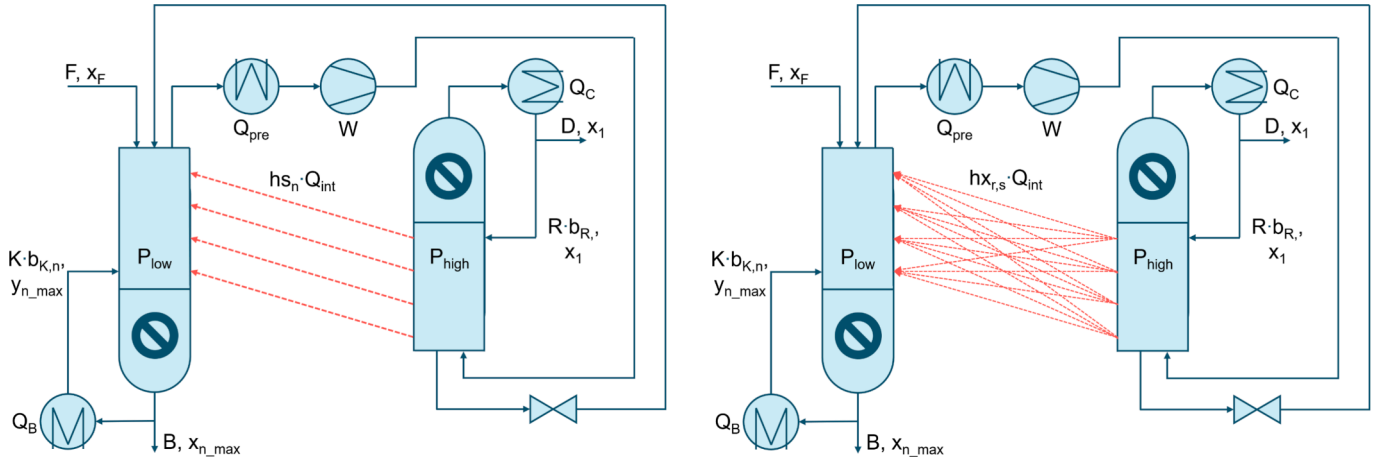

Fig. 7. Model of HIDiC in free structure with crossed out regions representing the non-physically meaningful stages showing possible locations for same-height (left) and variable-height (right) heat transfer.

conventional columns and the competing heat pump concept of VRC.

3.1. Comparison of same-height and variable-height heat transfer

To understand how different heat integration strategies compare in terms of computational effort and their impact on the resulting design and performance, the two HIDiC models with same-height heat transfer and variable-height heat transfer are first evaluated for the separation of a close boiling equimolar mixture of benzene-fluorobenzene with a boiling point difference of just 5.5 K. The optimization is performed for a superstructure model with a total number of 230 equilibrium stages (including the reboiler and condenser) equally distributed between the rectifying and stripping section. The respective HIDiC designs and the internal vapor flowrates obtained by the minimization of the TAC are illustrated in Fig. 8 for the same-height heat transfer model and Fig. 9 for the variable-height heat transfer model. The optimization with all steps of the solution strategy described in Section 2.3 is performed with a respective wall clock time of just 8:26 min for the same-height heat transfer model and 18:56 min for the variable-height model.

The optimization of the same-height model results in a very uneven distribution of the number of stages with 100 stages in the rectifying section and only 28 in the stripping section. Heat is integrated internally at two positions, transferring heat from the rectifying section to the stripping section at the 2nd and 28th stage, which are basically the top and bottom of the stripping section. The TAC of the design with same-height heat transfer is 548,100 €/year and the design with variable-height heat transfer costs 503,600 €/year, providing a cost saving potential of 8%.

In the case of variable-height heat transfer, only a single heat transfer location is selected, transferring heat form the top stage of the rectifying section to the bottom stage of the stripping section, which is infeasible in the same-height heat transfer model and approaches the design of VRC-assisted distillation. Both HIDiC designs do not require an additional reboiler, since all heat required at the bottom of the stripping section is provided by internal heat integration. A validation of the optimization results with a dedicated rigorous simulation model in Aspen Plus V12.1, set up with equivalent specifications is provided in the SI in section 4. In addition to the cost savings the variable-height heat transfer design also requires a 26% lower electricity demand, resulting in 26% lower annual operating costs and a smaller compressor. While the compression ratio is almost identical for both designs, the vapor flow rate that is compressed between the rectifying and stripping section is 26% lower for variable-height heat transfer, as shown in Fig. 8 and Fig. 9. Note that the considerable difference in the number of trays in the column sections results from the differences in relative volatility, as indicated in Fig. 15.

Since the integrated amount of heat is also 26% smaller for variable-height heat transfer and only requires a single instead of two internal heat exchangers in addition to 28% lower condenser duty, the capital cost for heat exchangers is 18% lower. The smaller column diameter, smaller compressor and cheaper heat exchangers overcompensate the additional cost for the increased number of stages (+40%) in the variable-height solution, resulting in 3% lower annual capital cost compared to same-height heat transfer.

The resulting design for the selected heat integration of the variable-height solution for the asymmetric temperature profile of the benzene-fluorobenzene mixture shown in Fig. 10 matches exactly the suggestions of Shenvi *et al.* [24], who recommended that the best position for internal heat integration for asymmetric temperature profiles, is between the top of the rectifying section and the bottom of the stripping section, approaching the design of a VRC. This location allows heat transfer to occur as close to the minimum temperature difference as possible, minimizing the exergy losses associated with heat transfer.

Since those stages are not at the same height, this connection is infeasible for the same-height model, which consequently derives another sub-optimal design. Still, the majority of heat is transferred to the bottommost stage of the stripping section in that case, just not from the very top of the rectifying section.

This comparison illustrates that the variable-height heat transfer model is more flexible and allows for the design of an energetically and economically more beneficial design for the separation of the selected mixture. This observation is expected, since the same-height heat transfer model only provides a restricted design space of the more flexible variable-height heat transfer model. Since the extra effort for optimizing the more complex model is well affordable, it is suggested to generally perform HIDiC designs on the basis of the flexible variable-height heat integration model without liming the design space to inferior same-height heat transfer locations.

3.2. Evaluation of heat transfer at every stage along column height

Instead of only using a few internal heat exchange locations, the original concept of internally HIDiC is based on integrating energy at every stage [19]. Shenvi *et al.* [24] suggested a specific strategy with four individual intermediate heat exchanger locations, that represent a compromise between same-height and variable-height heat transfer, for the separation of an equimolar benzene-toluene mixture. The strategy provides the same potential energy savings as an internally HIDiC according to Shenvi *et al.* [24]. Yet, these results are based solely on simulation studies and analysis of the temperature profiles rather than optimization of the respective designs.

To estimate the performance of an internally HIDiC, the same-height heat transfer scenario is modified such that heat transfer is enforced at all stages at the same height based on the pre-defined surface area for heat transfer. For this purpose, an identical internal heat exchange area is assigned to all stages, defined as a single decision variable with upper bounds of 1 m^2 and 10 m^2. The minimum temperature difference for heat transfer in Eq. (40) is set to an epsilon-value of just 0.001 K, allowing for a close approximation of the temperature profiles in both

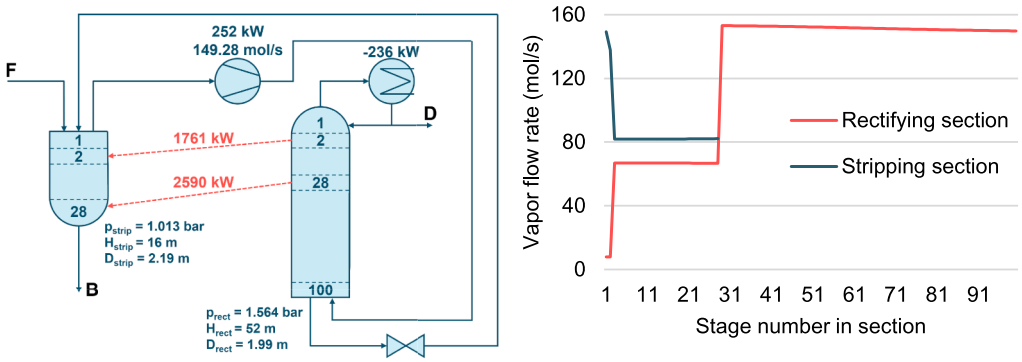

Fig. 8. Resulting HIDiC structure of TAC minimization and vapor flow rates for separation of equimolar benzene-fluorobenzene mixture using same-height heat transfer.

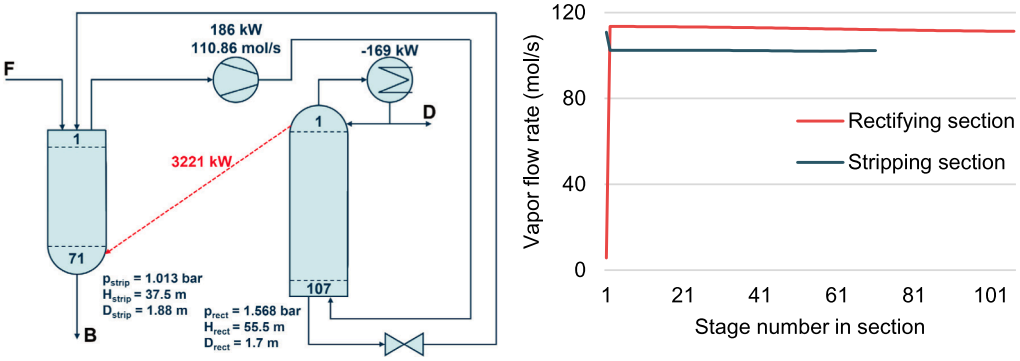

Fig. 9. Resulting HIDiC structure of TAC minimization and vapor flow rates for separation of equimolar benzene-fluorobenzene mixture using variable-height heat transfer.

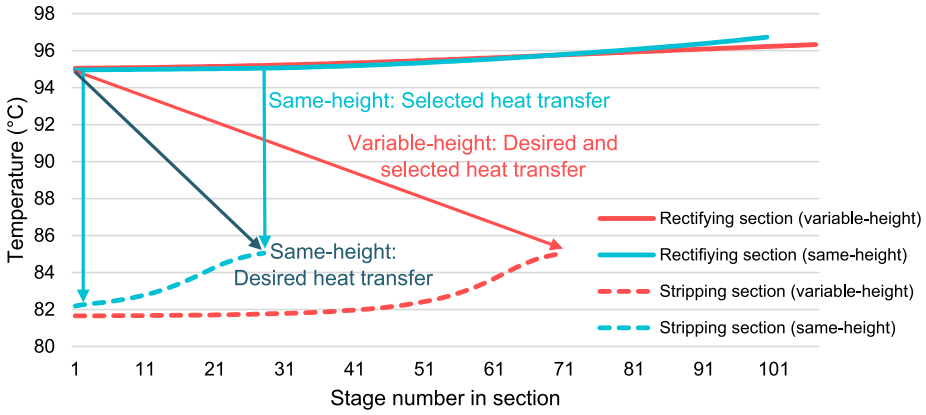

Fig. 10. Temperature profiles in column sections for both HIDiC heat transfer scenarios for separation of equimolar benzene-fluorobenzene mixture. Arrows indicate desired and selected heat transfer location.

sections. Although different designs for internally HIDiC have been proposed, including columns with partitioned walls, concentering columns and shell and tube designs [19], there are no specific equipment design and cost correlations for such specialized equipment available. Therefore, a pragmatic approach to evaluate the potential of such a specialized equipment is to focus solely on the possible reduction of the external energy demand that would be feasible in comparison to an externally HIDiC with few finite heat exchangers. Note that the external energy demand represents a net energy that does not differentiate between the type of required utilities. Electrical power to drive the compressor, which is pure exergy, is usually more valuable than steam at a certain temperature. The latter differentiation is reflected in the utility costs considered for the economic optimization discussed in section 3.4.

For this evaluation the separation of an equimolar benzene-toluene mixture is considered using a process structure with a fixed number of 50 stages in each section. For both cases, the optimized internally HIDiC designs, which are summarized in Table 2, make use of the upper bound of the heat exchange area, which is the only reasonable choice considering that the optimization focusses solely on the energy requirements and ignores the investment costs.

Table 2
Results of same-height heat transfer at every stage with constant heat transfer area for separation of equimolar benzene-toluene, optimized for external energy demand in fixed structure.

	1 m^2 on each stage	10 m^2 on each stage
Total external energy demand (kW)	171	168
Reboiler duty (kW)	140	144
Condenser duty (kW)	−149	−150
Preheater duty (kW)	0.7	0.37
Internally integrated heat (kW)	238	249
Compressor duty (kW)	30	24
Compression ratio	1.791	1.598

The resulting temperature differences for the internally HIDiC designs are in the range between 3.2 K and 7.6 K for 1 m^2 and between 0.12 K and 2.74 K for 10 m^2, for which only four of the internal heat exchangers exhibit temperature differences over 1 K. The fractional heat transfer and vapor flow rates for every stage in the internally HIDiC designs are shown in Fig. 11. Notably, the vapor flowrates do not exhibit sudden changes unlike for the TAC-optimal structures using variable-height and same-height heat transfer from Fig. 8 and Fig. 9. However, the vapor flowrates in both column sections are constantly changing to a significant extent, resulting in an increase of the vapor flowrate along the section height by a factor of 3. Such variations would definitely need to be compensated by a dedicated equipment design that balances the effective vapor loads along the column height. Especially for 10 m^2, many stages only integrate a very small fraction of the heat, due to the small temperature differences, which reduce exergy losses.

Comparing the energy-optimized performance of the internally HIDiC designs with the cost-optimized design of an externally HIDiC, based on the variable-height model, derived from a superstructure with an initial number of 50 stages in each section, it becomes however apparent that the potential benefits of the internally HIDiC are quite limited. The cost-optimized design is shown in Fig. 12. Despite the possibility for widely distributed heat transfer, heat is only transferred at two locations, which can easily be implemented by using conventional externally located heat exchangers.

Despite only using 23 stages in each section of the cost-optimized design, which is less than half that used in the minimum energy design of the internally HIDiC, the total external energy duty of 175 kW

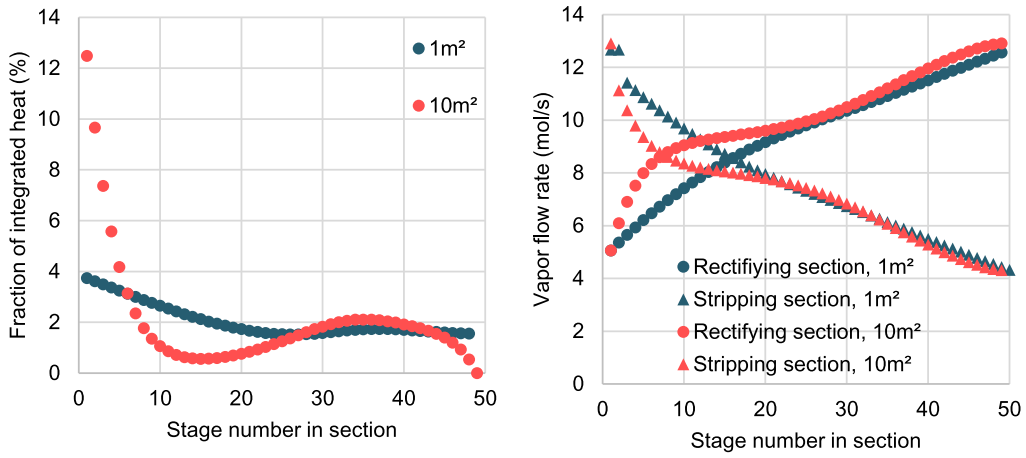

Fig. 11. Fraction of internal heat transfer (left) and vapor flow rates (right) for constant heat transfer area at every stage for separation of equimolar benzene-toluene, optimized for external energy demand in fixed structure.

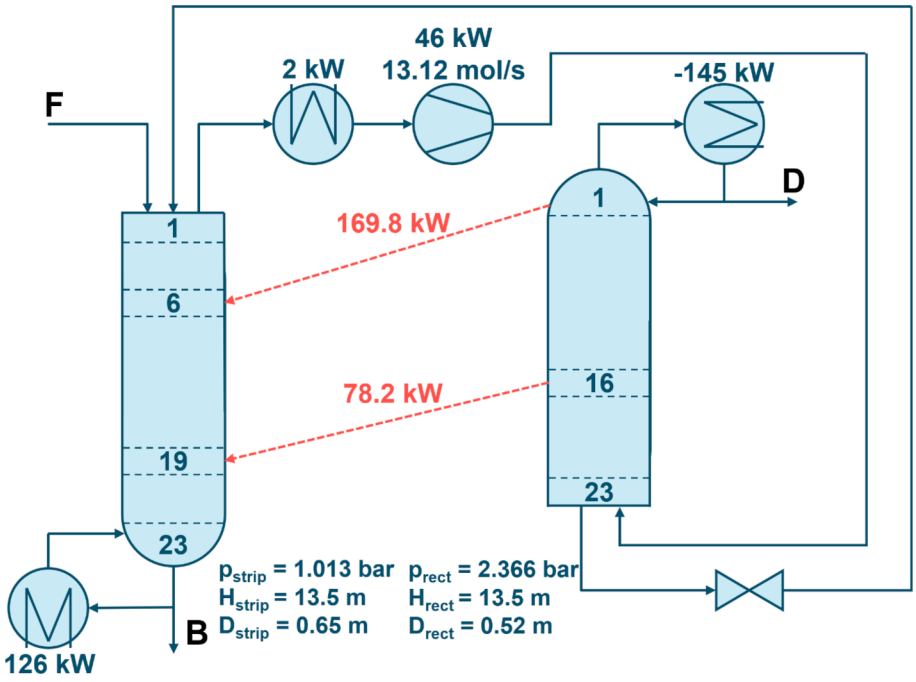

Fig. 12. Resulting HIDiC structure of TAC minimization for separation of equimolar benzene-toluene mixture using variable-height heat transfer.

is only 2.3% higher than the minimum energy requirement derived for the internally HIDiC with 1 m^2 of heat transfer area and 4.2% higher than the minimum energy duty for the internally HIDiC with 10 m^2 on each stage. This result confirms and strengthens previous conclusions on the limited potential of internal HIDiC designs [15,34], which reflect back on the practical implementations for which the only reported industrial implementation is an externally HIDiC with a finite number of few external heat exchangers [31]. Yet, such a comparison should of course be made on a case-specific basis, for which the proposed optimization models and solutions strategies provide an excellent tool to analyze specific separation problems and avoid any potentially misleading heuristics.

3.3. *Influence of number of internal heat exchange locations*

In order to investigate the influence of the specific number of heat exchange locations (without an upper bound on the heat exchanger area), the optimization of the variable-height heat transfer model is further evaluated for the separation of the equimolar benzene-toluene mixture regarding the minimization of the external energy demand with a fixed number of 50 stages in each column section.

Despite the possibility to transfer energy between an arbitrary number of stages, only six internal heat exchangers are selected as shown in Fig. 13 (left), whereas the majority of the heat is still transferred at the top and bottom ends of both sections.

With the aid of the additional constraints described in section 2.3.4, the number of internal heat exchangers is further constrained to one, two, and three individual locations, repeating the optimization with the fixed structure regarding the minimization of the external energy demand. Fig. 13 (right) shows that the total external energy demand increases by less than 4% even if only a single internal heat exchanger is used which transfers heat from the 31st stage of the rectifying section with the 27th stage of the stripping section, compared to the solution without constraints on the number of internal heat exchange locations. Therefore, limiting the number of heat exchange locations has a minuscule effect on the achievable external energy demand. This

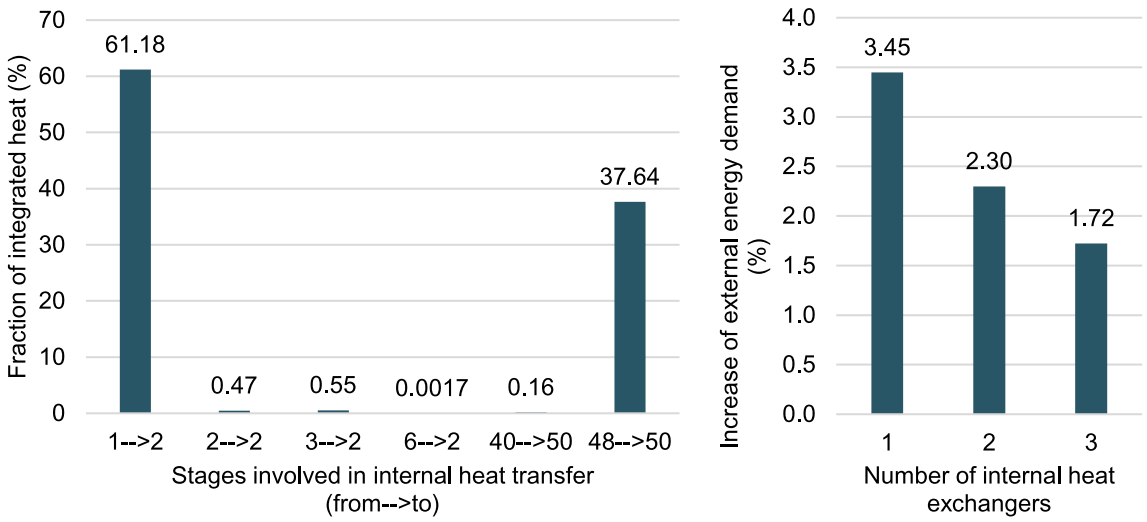

Fig. 13. Internal heat transfer locations for separation of equimolar benzene-toluene mixture optimized for external energy demand with fixed structure using variable-height heat transfer (left) and effect of limiting the number of internal heat excahnge locations (right).

matches the previously observed increase of less than 2% for four different ideal substance systems by Harwardt and Marquardt [15] when limited to three or less heat exchange positions. This is likely also the reason why the TAC-optimization only selects one or two heat exchangers, as the resulting design already exploits the majority of the possible heat integration.

Notably, fewer heat exchange locations result in higher compression ratios to achieve a large enough temperature difference for sufficient heat transfer: The compression ratio for six internal heat exchangers in the unconstrained scenario is 2.16, three exchangers result in a compression ratio of 2.4, two exchangers result in 2.45, and one exchanger results in a compression ratio of 2.83, which is an increase of about 30% compared to the design with 6 heat exchangers. In all cases, the reboiler duty supplies between 24% and 34% of the overall heat, indicating that a lower external energy demand is not feasible by providing all heat through heat integration, as this would increase the compressor or preheater duty.

Almost the entire energy saving potential can be exploited with as little as a single optimally located heat exchanger of conventional design like shell and tube. In combination with the conclusion of the previous section, it accordingly seems unreasonable to pursue the implementation of heat transfer along the height of the column, requiring much more complicated equipment which is still under development [29,62].

3.4. Comparison of HIDiC performance with VRC and conventional column

While many studies exemplify the large saving potential of HIDiC designs in combination with a conventional distillation column, it is essential to include the VRC-assisted distillation to this comparison, since any existing column can be retrofitted with VRC with little modification, while HIDiC designs are significantly more complex to implement. Therefore, the performance of a HIDiC design is next evaluated against that of a conventional column and a VRC-assisted column for the two previously evaluated separation problems. Table 3 summarizes the key results of all process design optimizations regarding the minimization of the TAC.

Both VRC and HIDiC use significantly less external energy than the conventional column for the separation of both mixtures. For the close-boiling mixture, the total external energy demand of VRC is 92% lower due to the significant reduction in reboiler duty by 97%. The energetic performance of the HIDiC design is even more impressive, as it reduces the external energy demand by 93%, which is 18% lower compared with the VRC. However, the VRC design is overall 15% less expensive. As

Table 3
Key results of TAC-optimal designs for different process alternatives for separation of equimolar close and wide boiling mixture.

Process	benzene-fluorobenzene (ΔT = 5.5 K)				benzene-toluene (ΔT = 30.5 K)		
	Conventional column	VRC	HIDiC (same-height)	HIDiC (variable-height)	Conventional column	VRC	HIDiC (variable-height)
Reboiler duty (kW)	2712	73	0	0	373	32	126
Condenser duty (kW)	−2707	−224	−236	−169	−369	−81	−145
Preheater duty (kW)	–	0	0	0	–	0	2
Internally integrated heat (kW)	–	2787	4347	3222	–	345	248
Compressor duty (kW)	–	155	252	186	–	54	46
Total external energy demand (kW)	2712	228	252	186	373	86	175
Reduction in external heat requirement (%)	–	97.3	100	100	–	91.4	65.7
Compression ratio	–	1.548	1.544	1.548	–	2.955	2.335
Flow rate through compressor (mol/s)	–	92.83	149.28	110.86	–	12.09	13.12
Number ofrectifying stages	137	104	100	107	16	14	23
Number ofstripping stages	54	44	28	71	16	15	23
Diameter (m)	1.705	1.751	1.99/2.194	1.702/1.877	0.619	0.622	0.524/0.645
Annual operating cost (k€/a)	1124.3	106.3	123.5	91.0	154.8	39.6	75.6
Annual capital cost (k€/a)	247.5	323.9	424.6	412.6	31.1	73.9	82.2
Total annual cost (k€/a)	1371.8	430.3	548.1	503.6	185.8	113.4	157.8
Computation time (min:s)	2:38	2:43	8:26	18:56	0:38	3:04	5:55

shown in Section 3.1, the HIDiC design does not require any external heat for the separation of the benzene-fluorobenzene mixture, such that all energy is supplied electrically, allowing for a design without a reboiler for fully electrified distillation. However, despite the validity of such a steady-state model, a design without an additional reboiler will likely be infeasible in operation, since the HIDiC can only be operated if a sufficient vapor stream is available that is further upgraded by the compressor. In contrast, the resulting VRC design is equipped with an additional reboiler for both mixtures. This is a result of the techno-economic optimization and the superstructure model, considering that the heat of condensation from the compressed vapor alone is insufficient to provide the required heat for evaporation, since the enthalpy of vaporization decreases at higher pressures. Apart from the additional reboiler, the excess heat could also be provided in the pre-heater or by means of an increased pressurization in the compressor, which are however both less economic, as also outlined in the study by Chen et al. [63]. Yet, the required excess heat may also be provided by integrating the vapor that is generated when expanding the condensed high-pressure stream in a flash unit or by integrating part of the heat from the condenser in the pre-heater [63,64] While not included in the current superstructure model, both options may further improve the performance of the VRC configuration and therefore do not alter the results of the current investigations. However, it is important to note that with these additional modifications a full electrification of the VRC design can be achieved.

The relative energy savings of both heat pump concepts, VRC and HIDiC, are less pronounced for the separation of the wide-boiling mixture due to the higher temperature difference which has to be overcome. This is of course to be expected. The absolute energy requirements are also lower for wide boiling systems than close boiling ones due to the easier separation. The optimized VRC design reduces the external energy demand by 77% and the external heat demand by 91% compared with the conventional column. While still outperforming the conventional column, the optimized HIDiC design (cf. Fig. 12) performs significantly worse than the VRC design with only a 53% reduction in total external energy, requiring four times as much external heat as the VRC. It is important to note that the overall heat demand of the HIDiC (376 kW) and the VRC (377 kW) is almost identical, but 34% of the heat for the HIDiC is provided externally with considerable costs for the required steam.

The reason for this difference is grounded in the potential heat that can be integrated in both designs. While the VRC design can exploit the heat of condensation for the top vapor stream leaving the column, which includes the reflux and the distillate product, the HIDiC design allows only for the integration of the heat of condensation for the internal reflux. The distillate has to leave the rectifying section as top vapor stream and is subsequently condensed in the external heat exchanger. The heat of condensation for the distillate is slightly higher than 140 kW, which is therefore a lower bound for the condenser duties of the HIDiC design (in case of no external reflux) and is closely approached in the results of both the same-height and variable height designs (cf. Table 2 and Fig. 14). This limitation of the HIDiC design can be overcome, if heat exchange is also allowed between the external condenser and the trays of the stripping section, or the external reboiler. However, this deviates from most of the equipment-integrated HIDiC concepts that have previously been discussed in literature [19] and is therefore not considered in the current work. After all, the current results highlight and explain this limitation of the HIDiC design, which is also reflected but not further analyzed in the results that were previously reported by Harwardt and Marquardt [15]. More importantly, this limitation is apparently not evident for the close-boiling benzene-fluorobenzene mixture, which requires a higher internal reflux, such that the compressor duty exceeds the condenser duty and provides sufficient energy surcharge to provide the total heat duty for the stripping section. Consequently, the extent to which this design limitation affects the energy requirements depends strongly on the specific separation problem.

The cost distribution for the derived designs is further illustrated in the bar graphs in Fig. 14. While the cost of the conventional columns are dominated by the cost of steam provision, the heat pump assisted distillation columns rely largely on electricity. This offers huge potential to effectively reduce the associated greenhouse gas emissions by not only reducing the net energy requirements, but also using green electricity. Especially for the separation of the narrow-boiling system, external steam use can be largely avoided. Despite higher investment costs, both heat pump assisted distillation column designs are economically viable under the considered economic scenario, with higher

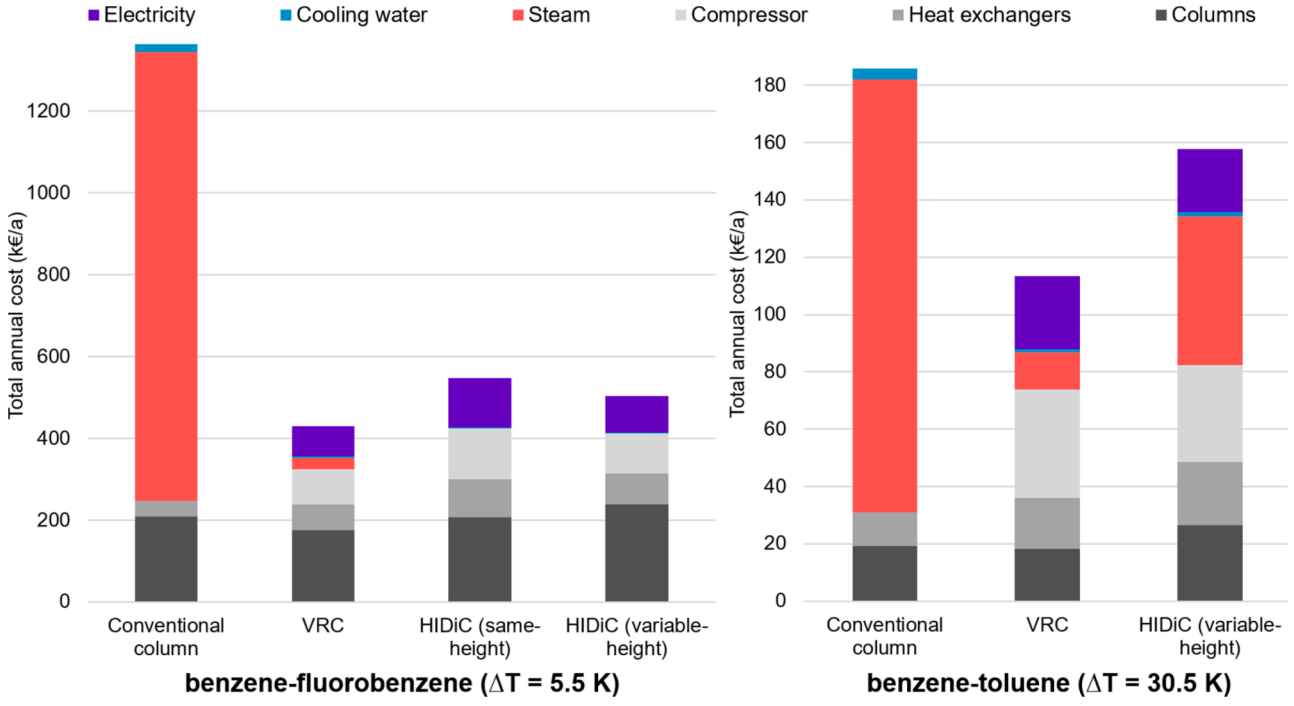

Fig. 14. TAC breakdown of TAC-optimal designs for different process alternatives for separation of equimolar close and wide boiling mixture.

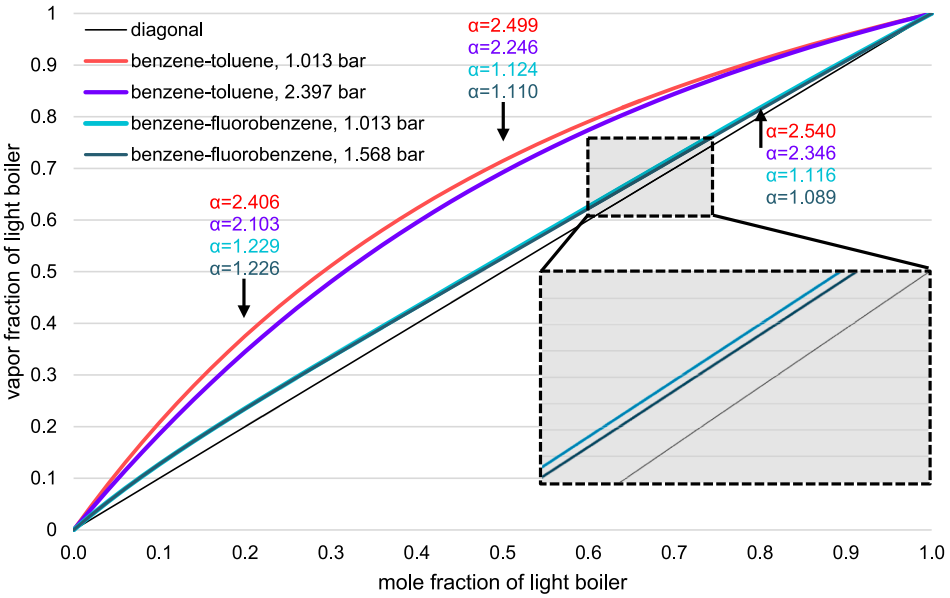

Fig. 15. x-y-diagram with relative volatility (α) for both substance systems with UNIQUAC at atmospheric pressure and the pressure of the rectifying section for HIDiC (variable-height).

savings for the close-boiling system, which is in line with the higher energy saving potential.

For both substance systems, the HIDiC is more expensive than VRC with a capital cost increase of 22% for the separation of the close-boiling mixture, for which the HIDiC design with variable-height heat transfer approaches the design of VRC by integrating all heat from the top of the rectifying section to the bottom of the stripping section (cf. Section 3.1). Therefore, both heat pump types need to overcome the same highest possible temperature difference for the given separation, resulting in nearly identical compression ratios of 1.548.

In addition to higher complexity of the HIDiC design, it also operates the rectifying section at increased pressure, reducing the driving force for separation for the considered case studies (cf. Fig. 15). Consequently, more stages and/or higher reflux and heat demand are required, which directly translates to larger vapor flow rates. Accordingly, the flow rate through the compressor is 19% higher for the HIDiC (110.86 mol/s) compared to the VRC-assisted column (92.83 mol/s), leading to 20% higher compression duty (HIDiC: 186 kW, VRC: 155 kW) and thus a 15% more expensive compressor. The HIDiC still requires 14% lower operating costs since no steam is required, but the TAC is 17% higher than for VRC-assisted column due to the higher investment cost. For the wide boiling mixture, the HIDiC design has 10% higher annual capital cost than the VRC-assisted design, but is overall almost 40% more expensive, due to the 91% higher operating cost grounded in the four times higher demand in external steam.

To summarize, both HIDiC and VRC-assisted column designs require significantly less external energy compared to conventional columns, resulting in much lower operating costs at higher capital expenses. Depending on the considered deprecation time and utility prices, both heat pump assisted designs can achieve substantially lower TAC than conventional columns, especially for the separation of close boiling systems. While it appears that the main advantage of the HIDiC design compared with VRC is a potentially lower compression ratio, especially recognized for wider boiling mixtures, the derived designs for minimized TAC perform even worse for in this case. If HIDiC can be economically competitive with VRC, it is likely only for very close boiling systems. The proposed optimization-based approach presents an effective tool to screen for possible applications and evaluate the specific benefits that may be offered by a dedicated HIDiC design.

4. Conclusion

To overcome the limited flexibility of previously proposed HIDiC design methods a novel modeling and solution approach for the optimization of HIDiC designs is presented in the current study. Two novel model formulations enable heat integration strategies between both sections either between stages at the same-height, regardless of the initial number of stages, as well as a flexible heat integration between any stages in the different sections. The composite modeling and solution strategy enables the computationally efficient solution of the complex MINLP problems with a significant number of decision variables, within wall clock times of less than 20 min on a common desktop computer even for superstructure models with more than 200 initial stages. The gradient-based optimization effectively overcomes the problem of an exponential increase in simulation effort for simulation-based optimization methods, and allows for further extensions of the design problem or the integration in multi-objective or stochastic optimization problems.

While the flexible superstructure model allows for general heat transfer between any stages in the rectifying and stripping section, all TAC-optimized designs utilize only few internal heat exchangers for both heat integration strategies, suggesting that more complex configurations with numerous heat exchangers do not provide additional economic benefits. The obtained results confirm that heat transfer at every stage along the column height offers only marginal energy savings given that a sufficiently large heat transfer area is provided. While both VRC and HIDiC outperform conventional columns and can be designed without the need for external heat at the reboiler, economically optimized solutions may still operate with some residual external heat. In both considered cases, the VRC design offers the economically more attractive solution.

While providing a more flexible HIDiC model that extends the design space beyond the previous model of Harwardt and Marquardt [15], providing improved designs, the current results support the initial conclusions that VRC designs are in most cases the better choice. The results reveal the apparent limitation of an equipment-integrated HIDiC design, which unlike the VRC-assisted distillation requires an external condenser for the condensation of the distillate, potentially resulting in the need for external steam provision. While this limitation can theoretically be overcome by allowing for direct heat transfer between the

condenser and reboiler in the HIDiC design, such design further approaches the VRC design providing little incentive for a significant improvement over VRC-assisted distillation.

Future research should further extend the evaluation to include other promising alternatives, including the aforementioned additional heat integration in the VRC design [63,64], as well as VRC-assisted distillation with intermediate heat exchangers [65] and closed-cycle heat pumps with selectable refrigerants. The latter can overcome the inherent limitation that the vapor in a distillation column may not be compressed due to safety considerations or unfavorable thermodynamics. Except for the study of Rix *et al.* [66], there is little current literature on the use of closed-cycle heat pumps in distillation processes despite their growing popularity in residential heating. While closed-cycle heat pumps do of course introduce additional losses due to the secondary heat exchanger the extended range of applications may result in an increased exploitation. A general improvement of the current models would include pressure drop computations, which are specifically relevant for vacuum distillation, as investigated by Rix *et al.* [66]. The consideration of additional pressure will also increase the cost for very narrow boiling systems that require high column sections, such as the benzene-fluorobenzene system.

Nomenclature

Symbol	Explanation
A_{int_HX}	Area of internal heat exchangers
b_F, b_R, b_K	binary decision variable of feed, reflux, boil-up
b_{K_Sum}, b_{R_Sum}	sum of b_K, sum of b_R
B	bottom flow rate
c_p	specific heat capacity
C_{inv}	total investment costs
C_{opt}	hourly operating costs
D	distillate flow rate
D_{column}	column diameter
$D_{rectifiying}$	diameter of rectifying section
$D_{stripping}$	diameter of stripping section
F	feed flow rate
h^L, h^V	liquid enthalpy, vapor enthalpy
h^V_{comp}	enthalpy of compressed vapor
h_{extra}	extra clearance space
h_{tray}	actual height of a single tray
hr_n, hs_n	heat transfer decision variable for the rectifying/stripping section
$hx_{r,s}$	specific relative amount of heat transfer between an individual pair of stages in the rectifying section and stripping section
i	interest rate, component index
K	boil-up flow rate
L	liquid flow rate
M	molar mass, penalty weighting factor
n	stage number
n_{actual}	actual number of stages
n_{max}	maximum number of stages
nhx_n, $nhx_{r,s}$	continuous variables for indication of presence of heat transfer
NHX	number of internal heat exchange locations
p	column pressure
p_F, p_R, p_K	Penalty term for decision variable of feed, reflux, boil-up
Q_{aux}	auxiliary condenser duty
Q_B, Q_C	reboiler duty, condenser duty
Q_{HI}	integrated duty for VRC
Q_{int}	overall internally transferred heat for HIDiC
Q_{pre}	preheater duty
Q_{tot}	total external energy demand
R	reflux flow rate
R_{gas}	universal gas constant
t	depreciation time
t_a	annual operating hours
T	temperature
$T_{compressed\ vapor}$	bubble point temperature of compressed vapor
ΔT_{min}	minimum temperature difference
T_{sat}	temperature of the saturated vapor
U	heat transfer coefficient
V	vapor molar flow
W	compressor work
x	mole fraction in liquid stream
y	mole fraction in vapor stream
κ	isentropic coefficient
$\eta_{isentropic}$	isentropic efficiency

(*continued on next column*)

(*continued*)

CRediT authorship contribution statement

Momme Adami: Conceptualization, Validation, Writing – original draft, Writing – review & editing, Visualization, Project administration, Methodology. **Kayenat Farheen:** Methodology, Software, Investigation, Validation, Writing – original draft. **Mirko Skiborowski:** Resources, Supervision, Writing – review & editing, Funding acquisition.

Declaration of competing interest

The authors declare that they have no known competing financial interests or personal relationships that could have appeared to influence the work reported in this paper.

Acknowledgements

The authors would like to acknowledge that the work that led to the writing of this article was funded by the Deutsche Forschungsgemeinschaft (DFG, German Research Foundation) – Projektnummer 523327609.

Appendix A. Supplementary material

Supplementary data to this article can be found online at https://doi.org/10.1016/j.seppur.2024.131061.

References

[1] L.C. Vieira, M. Longo, M. Mura, Are the European manufacturing and energy sectors on track for achieving net-zero emissions in 2050? An empirical analysis, *Energy Policy* 156 (2021) 112464, https://doi.org/10.1016/j.enpol.2021.112464.
[2] A. Marina, S. Spoelstra, H.A. Zondag, A.K. Wemmers, An estimation of the European industrial heat pump market potential, *Renewable and Sustainable Energy Reviews* 139 (2021) 110545, https://doi.org/10.1016/j.rser.2020.110545.
[3] T.J. Mathew, et al., Advances in distillation: Significant reductions in energy consumption and carbon dioxide emissions for crude oil separation, *Joule* 6 (11) (2022) 2500–2512, https://doi.org/10.1016/j.joule.2022.10.004.
[4] E.L. Cussler, B.K. Dutta, On separation efficiency, *AIChE J.* 58 (12) (2012) 3825–3831, https://doi.org/10.1002/aic.13779.
[5] A.A. Kiss, R. Smith, Rethinking energy use in distillation processes for a more sustainable chemical industry, *Energy* 203 (2020) 1–12, https://doi.org/10.1016/j.energy.2020.117788.
[6] M. Skiborowski, K. F. Kruber, and T. Waltermann, "Sustainable Distillation Processes," in *Sustainable Separation Engineering*, G. Szekely and D. Zhao, Eds.: Wiley, 2022, pp. 431–481.
[7] M. Jobson, "Energy Considerations in Distillation," in *Distillation*, Elsevier (2014) 225–270.
[8] M. Blahušiak, A.A. Kiss, S. Kersten, B. Schuur, Quick assessment of binary distillation efficiency using a heat engine perspective, *Energy* 116 (2016) 20–31, https://doi.org/10.1016/j.energy.2016.09.097.
[9] M. Skiborowski, Synthesis and design methods for energy-efficient distillation processes, *Current Opinion in Chemical Engineering* 42 (2023) 100985, https://doi.org/10.1016/j.coche.2023.100985.
[10] R.T. Gooty, J.A.C. Velasco, R. Agrawal, Methods to assess numerous distillation schemes for binary mixtures, *Chemical Engineering Research and Design* 172 (2021) 1–20, https://doi.org/10.1016/j.cherd.2021.05.022.
[11] A.K. Jana, Advances in heat pump assisted distillation column: A review, *Energy Conversion and Management* 77 (2014) 287–297, https://doi.org/10.1016/j.enconman.2013.09.055.
[12] C. Cui, et al., Electrification of distillation for decarbonization: An overview and perspective, *Renewable and Sustainable Energy Reviews* 199 (2024) 114522, https://doi.org/10.1016/j.rser.2024.114522.
[13] Z. Mekidiche, J.A. Labarta, J. Javaloyes-Anton, J.A. Caballero, From power to heat: Strategies for electrifying distillation for sustainable chemical processes, *Applied Thermal Engineering* 257 (2024) 124316, https://doi.org/10.1016/j.applthermaleng.2024.124316.

[14] O. Annakou, P. Mizsey, Rigorous investigation of heat pump assisted distillation, *Heat Recovery Systems and CHP* 15 (3) (1995) 241–247.
[15] A. Harwardt, W. Marquardt, Heat-integrated distillation columns: Vapor recompression or internal heat integration? *AIChE J.* 58 (12) (2012) 3740–3750, https://doi.org/10.1002/aic.13775.
[16] X. You, I. Rodriguez-Donis, V. Gerbaud, Reducing process cost and CO2 emissions for extractive distillation by double-effect heat integration and mechanical heat pump, *Applied Energy* 166 (2016) 128–140, https://doi.org/10.1016/j.apenergy.2016.01.028.
[17] H. Cong, J.P. Murphy, X. Li, H. Li, X. Gao, Feasibility Evaluation of a Novel Middle Vapor Recompression Distillation Column, *Ind. Eng. Chem. Res.* 57 (18) (2018) 6317–6329, https://doi.org/10.1021/acs.iecr.8b00038.
[18] J. Fang, X. Cheng, Z. Li, H. Li, C. Li, A review of internally heat integrated distillation column, *Chinese Journal of Chemical Engineering* 27 (6) (2019) 1272–1281, https://doi.org/10.1016/j.cjche.2018.08.021.
[19] A.A. Kiss, Z. Olujić, A review on process intensification in internally heat-integrated distillation columns, *Chemical Engineering and Processing: Process Intensification* 86 (2014) 125–144, https://doi.org/10.1016/j.cep.2014.10.017.
[20] R.S.H. Mah, J.J. Nicholas, R.B. Wodnik, Distillation with secondary reflux and vaporization: A comparative evaluation, *AIChE J* 23 (5) (1977) 651–658, https://doi.org/10.1002/aic.690230505.
[21] G.G. Haselden, An approach to minimum power consumption in low temperature gas separation, *Chemical Engineering Research and Design* 36 (1958) 123–132.
[22] M. Nakaiwa, K. Huang, A. Endo, T. Ohmori, T. Akiya, T. Takamatsu, Internally heat-integrated distillation columns: a review, *Chemical Engineering Research and Design* 81 (1) (2003) 162–177.
[23] J. Koehler, P. Poellmann, E. Blass, A Review on Minimum Energy Calculations for Ideal and Nonideal Distillations, *Ind. Eng. Chem. Res.* 34 (4) (1995) 1003–1020, https://doi.org/10.1021/ie00043a001.
[24] A.A. Shenvi, D.M. Herron, R. Agrawal, Energy Efficiency Limitations of the Conventional Heat Integrated Distillation Column (HIDiC) Configuration for Binary Distillation, *Ind. Eng. Chem. Res.* 50 (1) (2011) 119–130, https://doi.org/10.1021/ie101698f.
[25] B. Linnhoff, H. Dunford, R. Smith, Heat integration of distillation columns into overall processes, *Chemical Engineering Science* 38 (8) (1983) 1175–1188.
[26] A.K. Jana, Heat integrated distillation operation, *Applied Energy* 87 (5) (2010) 1477–1494, https://doi.org/10.1016/j.apenergy.2009.10.014.
[27] M. Gadalla, L. Jiménez, Z. Olujic, and P. & Jansens, "A thermo-hydraulic approach to conceptual design of an internally heat-integrated distillation column (i-HIDiC)," *Computers & Chemical Engineering*, 31(10), pp. 1346–1354, 2007.
[28] K. Matsuda, K. Iwakabe, M. Nakaiwa, Recent Advances in Internally Heat-Integrated Distillation Columns (HIDiC) for Sustainable Development, *J. Chem. Eng. Japan* 45 (6) (2012) 363–372.
[29] M. Marin-Gallego, B. Mizzi, D. Rouzineau, C. Gourdon, M. Meyer, Concentric Heat Integrated Distillation Column (HIDiC): a new specific packing design, characterization and pre-industrial pilot unit validation, *Chemical Engineering and Processing: Process Intensification* 171 (2022) 108643, https://doi.org/10.1016/j.cep.2021.108643.
[30] O. Bruinsma, et al., The structured heat integrated distillation column, *Chemical Engineering Research and Design* 90 (4) (2012) 458–470, https://doi.org/10.1016/j.cherd.2011.08.023.
[31] T. Wakabayashi, K. Yoshitani, H. Takahashi, S. Hasebe, Verification of energy conservation for discretely heat integrated distillation column through commercial operation, *Chemical Engineering Research and Design* 142 (2019) 1–12, https://doi.org/10.1016/j.cherd.2018.11.031.
[32] Koch-Glitsch, *SUPERHIDIC Technology*. Accessed: Nov. 8 2024. [Online]. Available: https://www.koch-glitsch.com/services/process-systems/superhidic-technology?servicecategory=Process-Systems&service=true&level=2.
[33] T. Wakabayashi, S. Hasebe, Design of heat integrated distillation column by using H-xy and T-xy diagrams, *Computers & Chemical Engineering* 56 (2013) 174–183, https://doi.org/10.1016/j.compchemeng.2013.05.020.
[34] B. Suphanit, Optimal heat distribution in the internally heat-integrated distillation column (HIDiC), *Energy* 36 (7) (2011) 4171–4181, https://doi.org/10.1016/j.energy.2011.04.026.
[35] R. Gutiérrez-Guerra, R. Murrieta-Dueñas, J. Cortez-González, J.G. Segovia-Hernández, S. Hernández, A. Hernández-Aguirre, Design and optimization of HIDiC columns using a constrained Boltzmann-based estimation of distribution algorithm-evaluating the effect of relative volatility, *Chemical Engineering and Processing: Process Intensification* 104 (2016) 29–42, https://doi.org/10.1016/j.cep.2016.02.004.
[36] M.A. Gadalla, Internal heat integrated distillation columns (iHIDiCs)—New systematic design methodology, *Chemical Engineering Research and Design* 87 (12) (2009) 1658–1666, https://doi.org/10.1016/j.cherd.2009.06.005.
[37] H. Shahandeh, J. Ivakpour, N. Kasiri, Internal and external HIDiCs (heat-integrated distillation columns) optimization by genetic algorithm, *Energy* 64 (2014) 875–886, https://doi.org/10.1016/j.energy.2013.10.042.
[38] P. Qiu, B. Huang, Z. Dai, F. Wang, Data-driven analysis and optimization of externally heat-integrated distillation columns (EHIDiC), *Energy* 189 (2019) 116177, https://doi.org/10.1016/j.energy.2019.116177.
[39] J.R.R.A. Martins, A. Ning, *Engineering Design Optimization*, Cambridge University Press, 2022.
[40] B. Gross, P. Roosen, Total process optimization in chemical engineering with evolutionary algorithms, *Computers & Chemical Engineering* 22 (1998) S229–S236, https://doi.org/10.1016/S0098-1354(98)00059-3.
[41] T. Janus, et al., Optimization-Based Process Synthesis Based on a Commercial Flowsheet Simulator, *Chemie Ingenieur Technik* 89 (5) (2017) 655–664, https://doi.org/10.1002/cite.201600179.
[42] J.R. Alcántara-Avila, S. Hasebe, M. Kano, New Synthesis Procedure To Find the Optimal Distillation Sequence with Internal and External Heat Integrations, *Ind. Eng. Chem. Res.* 52 (13) (2013) 4851–4862, https://doi.org/10.1021/ie302863p.
[43] R. Gutiérrez-Guerra, J.G. Segovia-Hernández, Novel approach to design and optimize heat-integrated distillation columns using Aspen Plus and an optimization algorithm, *Chemical Engineering Research and Design* 196 (2023) 13–27, https://doi.org/10.1016/j.cherd.2023.06.015.
[44] J. Viswanathan, I.E. Grossmann, A combined penalty function and outer-approximation method for MINLP optimization, *Computers & Chemical Engineering* 14 (7) (1990) 769–782, https://doi.org/10.1016/0098-1354(90)87085-4.
[45] M. Skiborowski, A. Harwardt, W. Marquardt, Efficient optimization-based design for the separation of heterogeneous azeotropic mixtures, *Computers & Chemical Engineering* 72 (5) (2015) 34–51, https://doi.org/10.1016/j.compchemeng.2014.03.012.
[46] T. Waltermann, M. Skiborowski, Conceptual Design of Highly Integrated Processes - Optimization of Dividing Wall Columns, *Chemie Ingenieur Technik* 89 (5) (2017) 562–581, https://doi.org/10.1002/cite.201600128.
[47] R.C. Pattison, C. Tsay, M. Baldea, Pseudo-transient models for multiscale, multiresolution simulation and optimization of intensified reaction/separation/recycle processes: Framework and a dimethyl ether production case study, *Computers & Chemical Engineering* 105 (2017) 161–172, https://doi.org/10.1016/j.compchemeng.2016.12.019.
[48] T. Waltermann, M. Skiborowski, Efficient optimization-based design of energy-integrated distillation processes, *Computers & Chemical Engineering* 129 (8) (2019) 106520, https://doi.org/10.1016/j.compchemeng.2019.106520.
[49] T. Waltermann, T. Grueters, D. Muenchrath, M. Skiborowski, Efficient optimization-based design of energy-integrated azeotropic distillation processes, *Computers & Chemical Engineering* 133 (2020) 106676, https://doi.org/10.1016/j.compchemeng.2019.106676.
[50] K. Kraemer, S. Kossack, W. Marquardt, Efficient Optimization-Based Design of Distillation Processes for Homogeneous Azeotropic Mixtures, *Ind. Eng. Chem. Res.* 48 (14) (2009) 6749–6764, https://doi.org/10.1021/ie900143e.
[51] D. Chen, X. Yuan, L. Xu, K.T. Yu, Comparison between Different Configurations of Internally and Externally Heat-Integrated Distillation by Numerical Simulation, *Ind. Eng. Chem. Res.* 52 (16) (2013) 5781–5790, https://doi.org/10.1021/ie400112k.
[52] T. Waltermann, S. Sibbing, M. Skiborowski, Optimization-based design of dividing wall columns with extended and multiple dividing walls for three- and four-product separations, *Chemical Engineering and Processing - Process Intensification* 146 (40) (2019) 1–18, https://doi.org/10.1016/j.cep.2019.107688.
[53] I.J. Halvorsen, S. Skogestad, Minimum Energy Consumption in Multicomponent Distillation. 1. Vmin Diagram for a Two-Product Column, *Ind. Eng. Chem. Res.* 42 (3) (2003) 596–604, https://doi.org/10.1021/ie010863g.
[54] K.M. Guthrie, Data and techniques for preliminary capital cost estimating, *Chemical Engineering* 76 (1969) 114–142.
[55] L.T. Biegler, I.E. Grossmann, A.W. Westerberg, *Systematic Methods of Chemical Process Design*, Upper Saddle River, New Jersey, 1997.
[56] S. Kossack, K. Kraemer, W. Marquardt, Efficient Optimization-Based Design of Distillation Columns for Homogenous Azeotropic Mixtures, *Ind. Eng. Chem. Res.* 45 (25) (2006) 8492–8502, https://doi.org/10.1021/ie060117h.
[57] M. Assaoui, B. Benadda, M. Otterbein, Distillation under High Pressure: A Behavioral Study of Packings, *Chem Eng & Technol* 30 (6) (2007) 702–708, https://doi.org/10.1002/ceat.200600173.
[58] J. Chen, Logarithmic mean: Chen's approximation or explicit solution? *Computers & Chemical Engineering* 120 (2019) 1–3, https://doi.org/10.1016/j.compchemeng.2018.10.002.
[59] M. Skiborowski, M. Rautenberg, W. Marquardt, A Hybrid Evolutionary–Deterministic Optimization Approach for Conceptual Design, *Ind. Eng. Chem. Res.* 54 (41) (2015) 10054–10072, https://doi.org/10.1021/acs.iecr.5b01995.
[60] K.F. Kruber, T. Grueters, M. Skiborowski, Advanced hybrid optimization methods for the design of complex separation processes, *Computers & Chemical Engineering* 147 (2021) 107257, https://doi.org/10.1016/j.compchemeng.2021.107257.
[61] R. Turton, R. C. Bailie, W. B. Whiting, and J. A. Shaeiwitz, *Analysis, synthesis, and design of chemical processes,* 3rd ed. Upper Saddle River, New Jersey: Pearson Education [distributor], 2009.
[62] M. Meyer, B. Mizzi, R. David, and Y. Omar, "Heat Integrated Distillation Column (Hidic): Experimental Study on a New Concentric Column Technology," *Chemical Engineering Transactions*, vol. 69, 2018.
[63] L. Chen, Q. Ye, Z. Jiang, J. Yuan, H. Zhang, N. Wang, Novel methodology for determining the optimal vapor recompressed assisted distillation process based on economic and energy efficiency, *Separation and Purification Technology* 251 (2020) 117393, https://doi.org/10.1016/j.seppur.2020.117393.
[64] A.S. Nogaja, M. Tawarmalani, R. Agrawal, Cogeneration Improves Separation Efficiency, *Ind. Eng. Chem. Res.* 63 (43) (2024) 18564–18574, https://doi.org/10.1021/acs.iecr.4c03190.
[65] M. Skiborowski, K.F. Kruber, "Exergy-based optimization for the synthesis of heat pump assisted distillation columns," in *Computer Aided Chemical Engineering, 34th European Symposium on Computer Aided Process Engineering / 15th International Symposium on Process Systems Engineering*: Elsevier, 2024, pp. 1351–1356.
[66] A. Rix, M. Schröder, N. Paul, Vapor recompression: An interesting option for vacuum columns? *Chemical Engineering Research and Design* 191 (2023) 226–235, https://doi.org/10.1016/j.cherd.2023.01.030.